Capturing features of hourly-resolution energy models through statistical annual indicators

Gonzalo Parrado-Hernando[*]
Department of System Engineering and Automation
School of Industrial Engineering, University of Valladolid, Spain
e-mail: gonzalo.parrado@uva.es

Luka Herc
Department of Energy, Power Engineering and Environment
Faculty of Mechanical Engineering and Naval Architecture
University of Zagreb, Zagreb, Croatia
e-mail: luka.herc@.fsb.hr

Antun Pfeifer
Department of Energy, Power Engineering and Environment
Faculty of Mechanical Engineering and Naval Architecture
University of Zagreb, Zagreb, Croatia
e-mail: Antun.Pfeifer@fsb.hr

Iñigo Capellán-Perez
Department of System Engineering and Automation
School of Industrial Engineering, University of Valladolid, Spain
e-mail: inigo.capellan@uva.es

Ilija Batas Bjelić
Institute of Technical Sciences of Serbian Academy of Sciences and Arts, Belgrade, Serbia, Serbia
e-mail: ilija.batas-bjelic@itn.sanu.ac.rs

Neven Duić
Department of Energy, Power Engineering and Environment
Faculty of Mechanical Engineering and Naval Architecture
University of Zagreb, Zagreb, Croatia
e–mail: Neven.Duic@fsb.hr

Fernando Frechoso-Escudero
Department of Electrical Engineering
School of Industrial Engineering, University of Valladolid, Spain
e-mail: frechoso@eii.uva.es

Luis Javier Miguel González
Department of System Engineering and Automation
School of Industrial Engineering, University of Valladolid, Spain
e-mail: ljmiguel@eii.uva.es

[*] Corresponding author.

Vladimir Z. Gjorgievski
Faculty of Electrical Engineering and Information Technologies, Ss. Cyril and Methodius University in Skopje, North Macedonia
e-mail: vladimir.gjorgievski@feit.ukim.edu.mk

ABSTRACT

Long term-energy planning has gradually moved towards finer temporal and spatial resolutions of the energy system to design the decarbonization of the society. However, integrated assessment models (IAMs), focusing on a broader concept of sustainability transition, are typically yearly-resolution models which complicates capturing the specific supply-demand dynamics, relevant in the transition towards renewable energy sources (RES). Different methods for introducing sub-annual information are being used in IAMs, but the hourly representation of variable RES remains challenging.

This article presents a method to translate the main dynamics of an hourly-resolution energy model into a yearly-resolution model. Here we test our method with the current European Union region (EU-27) by configuring and applying the hourly-resolution EnergyPLAN. Multiple linear regression analysis is applied to 174960 simulations (set by varying 39 inputs by clusters and reaching 100% renewable systems), relating the adjusted capacity factors of the technologies as well as the variation of electricity demand and natural gas consumption as a function of the options installed to manage the variable RES. The obtained results allow validation of the developed approach, which shows to be flexible and easily generalizable enough to be applied to any couple of hourly and annual-resolution models and/or country.

KEYWORDS

EnergyPLAN, Integrated Assessment Model (IAM), 100% renewables, Variable Renewable Energy Source (VRES).

1. INTRODUCTION

The European Union (EU) stipulates that achieving a climate-neutral economy will allow the EU to evolve into an equitable and sustainable society with a cutting-edge and vibrant economy [1]. To achieve the goals, remarkable progress has been made by expanding the exploitation of renewable sources of energy, "*from a technology, resource assessment, and system design perspective'* [2], primarily due to their reduced cost of electricity generation – particularly wind and solar technologies – and ongoing research to improve their characteristics [3]. However, fostering the use of renewables to reduce the annual net carbon footprint radically changes the traditional technical and market operations of the energy system due to their variable nature. Especially, the power system needs an adaptation to new technical [4][5], economic [6]–[8] and regulatory conditions [9], among others [10]. Last but not least, dispatchable renewables could relax a situation by imitating the traditional dispatchable fossil-fuelled technology [11].

To mathematically test and assess national and international policies in the context of the energy transition, it is fundamental and calls for adequate computer tools to design it. From the set of models available, the IAMs have been traditionally (since the 1970s) used to increase the awareness of the synergies between elements. Summarizing an introduction written by Nordhaus [12], an IAM may be defined as a computational shared framework of applied knowledge (effective understanding) to realistically represent the internal structural behavior of the human-Earth system and assess the best policies (i.e., those causing the desired effects) to be implemented in our society. The interdisciplinarity covers diverse fields from natural sciences and economics to sociology and law, and researchers propose their modeling in different programming languages (GAMS – Generalized Algebraic Modeling System – [13], Vensim [14]), modeling approaches (general and partial equilibrium [15], system dynamics [14], agent-based [16]) and, more recently, open platforms (GAMS/Java/Python/R) to further facilitate the collaborative work and communication between the database, the graphical user interface, and the analysis of results that scientists and policy makers claim for so much [17]. J. Weyant classifies the contributions of IAM in the literature about human development and energy transitions [18]. In this reference, the author states that *"IAMs differ tremendously in their level of detail and the complexity and interconnections they consider"*. Given the scope and influence in the Intergovernmental Panel on Climate Change (IPCC) reports (working group 3 [19]), an ethical discussion is present to support the transparency and high standards of science in this influencing field [20][21].

For policy makers to assess energy transitions, variable renewable energy sources – wind onshore, wind offshore, solar-PV, run-of-river hydropower, wave, and tidal marine power – as well as the energy demand requires *enough* temporal detail in IAMs. The next subsection briefly discusses a literature review of the methods used in the IAMs to represent the renewable and demand variabilities in the power system (summarizing tables in APPENDIX A, which also includes the acronyms of the referenced models). Then, additional paragraphs about machine learning methods introduce the developed method with which this article aims to contribute to the field.

Large models such as IAMs face two overlapping problems to have a computationally and tractable hourly analysis of the energy system in the code. On the one hand, the lack of databases to study the fluctuations in time and space, for both supply and demand sides, and considering interannual variabilities [22]. On the other hand, the computational cost should be as low as possible to be used as a manageable product by policy makers and stakeholders. Consequently, the methods should be evaluated to have a manageable product while retaining the relevant details. Stephan Pfenninger [22] has evaluated some techniques to reduce the time resolution of this problem, however, *"there is no one-size-fits-all approach to reduce time resolution while also covering long-term variability"*.

1.1. Approaches in IAMs

The oldest type of method is related to time slices. These calculate the variables of interest for some representative days, as windows of the high resolution of the year, to then extrapolate the results standardly to the whole year. Time slices were pioneer methods to represent the variability of renewables and load demand in IAMs [23].

Similarly, the time-aggregation methods start with the lowest scale (e.g., 8760 hours) to then create composite results at the yearly level. Nowadays, the most used is based on the residual load duration curves (RLDC) [24]. The core idea of the RLDC approach is the calculation of the residuals by subtracting, hour by hour, the production of the non-dispatchable renewables from the electricity demand. After that, the rest of the technologies are allocated to completely match demand and supply, according to some restrictions such as the maximum gradient of the curve and the maximum capacity factor of the power units. However, the dynamics over consecutive hours are lost when residuals are sorted to create the curve from which electricity is allocated in the market. This produces some drawbacks such as the loss of information about hourly ramps up and down in the capacities, or the representation of seasonal variables. The RLDC method – as well as other stylized approaches – is based on parametric equations, an aspect that makes it computationally faster than soft- and hard-linking. The speed of doing calculations exponentially increases in relevance when IAMs deal with several modules, regions, and decades of simulation. The collection of features requires time balancing across modules to deliver a manageable product. Years later, some of the original authors studied how this method had influenced the IAM field, showing positive feedback in AIM/CGE, IMAGE, MESSAGE, POLES, and REMIND, at different levels of importance, to *"describe the fundamental dynamics of the power sector and the effect of VRE"* [25].

A different perspective may be enclosed within the so-called stylized approach, which consists of a set of equations to deliver results as similar as possible to the original model. The last one with a greater definition of the problem. The materials to calibrate the equations are the own results of the model to be simplified, so the information is condensed to have implicit knowledge in the upper-scale model.

Finally, the concept of soft- and hard-linking means the coherent joining of two or more codes to capture different details present in their frameworks, to increase the strength of the assessment. *Soft* and *hard* linking differ in the inexistence (*soft*) or existence (*hard*) of feedback communication while the simulation is running. The five integrated assessment models working with the shared socioeconomic pathways (SSPs), two novel IAMs (MEDEAS, WITCH-GLOBIOM), and an energy model (POLES) have been analyzed in this article (APPENDIX A) to overview the representation of variable RES in three aspects: potential production, power system operation, and flexibility options considered.

A heterogenous point of view has developed the methods to capture the technical structure, the economic structure, or a combination of two to represent the power system. POLES has evidenced greater detail than the other models. A recent comparative analysis [26] between simplified approaches and an hourly energy model concludes that IAMs could be criticized for underestimating fundamental effects when calculating the carbon removal demand, especially in the power system, given the large role of the variable renewables in most of the scenarios. The effects were hourly studied by Hoevenaars et al. [27], however, the research could not recommend a specific time unit in general. Very recently, another methodological review [28] concludes that the accuracy of time-series aggregation, i.e., to represent a period selection through temporal resolution reduction, is higher than approaches based on time slides. Even if both achieve a great reduction of computational cost, the first type of method delivers negligible differences in the energy mix, cost, emissions, and curtailment for resolutions below the 8 hours. Even if both achieve a great reduction of computational cost, the first type of method delivers negligible differences in the energy mix, cost, emissions, and curtailment for resolutions below the 8 hours. However, the time steps were included in a potential series of ratio 2, i.e., 2 hours, 4 hours, and 8 hours. So, the Authors did not calculate the optimal resolution time according to energy system characteristics.

On the one hand, soft-linking has been proved in OSeMOSYS (Open Source Energy Modelling System), a long-term planning energy model, [29]. On the other hand, the results of previous research with TIMES-PLEXOS (where TIMES means The Integrated MARKAL-EFOM System) allowed for implementing operational constraints to enhance OSeMOSYS [30]. For the same time scale (year), the enhanced OSeMOSYS model achieved a better allocation of the supply capacities (21.4%), and appreciable changes in the scenario to 2050 (14.1% higher capacity and 14.5% higher investments than the starting version of the model) [31].

Pietzcker et al. [25] have cross-validated 18 features of the power system present in six IAMs. The reference was REMIx, an hourly, nodal, and economic-based optimization power system model ([32]). The historical "utilization effect" (reduction in the capacity factor of the installed thermal, hydro, and storage power units) was well-captured by REMIND 1.6. All the IAMs underestimated the curtailment (figure 4, left, in [25]) while revealing 40-50% higher storage capacity.

The only study of hard-linking between an IAM (MESSAGEix-GLOBIOM) and a power system model (PLEXOS-World) has been recently published [33]. Key mechanisms of this framework are the temporal demand downscaling, the special capacity downscaling, a long-term capacity expansion, and the integration of inter-regional trade. However, the energy models are usually more developed. For instance, TIMES ([34][35]) and EnergyPLAN, both long-term planning energy models, have been combined to study the continental Portugal energy system for the period 2005-2050. Compared to TIMES without EnergyPLAN, the integration of electricity overproduction was around 79% higher and the results showed significant differences in the requirements of storage [36].

Also to TIMES, PLEXOS has been connected to improve the reliability of the Irish power system results [37]. This power system model is based on linearised real power flows and assumes that voltages are all 1 p.u. [38], so every year simulated with PLEXOS cost more than five hours, while 40 seconds for a year of TIMES. However, 8% of curtailment and 21% of gas consumption for combined-cycle units are estimated by TIMES-PLEXOS, where TIMES was estimating 0% for both outputs (Table 5 of the reference).

Table A. *1* summarizes the methods used in IAMs. POLES seems to be the most complete IAM. This model also contains the highest number of flexibility options (Table A. *2*). The back-up facilities to guarantee the supply are represented in all the IAMs, but the options so-called demand-side management, vehicle-to-grid capacity, and power-to-heat are only in this one. Technically, the soft-linking between MESSAGEix and GLOBIOM achieves powerful details in the power system to assess the reliability of real power flows in the grid.

1.2. Machine learning algorithms

Consequently, the issue is therefore rooted in the hourly resolution, which can be achieved by an energy model. So, this paper aims to offer a stylized mathematical approach to represent the connection between inputs and outputs while considering as many hourly effects provoked by variable RES in the energy system as possible, easy to be interpreted and assuming a low or inexpensive computational effort, and easily integrable into different codes and frameworks.

The developed method of this work consists of performing combinations in the energy model, using the results to condense the hourly information into annual relationships. Peter Harrington [39] introduces the machine learning world to solve a broad set of problems. Since the labels and target values of inputs and outputs are known, the searching is focused on the so-called supervised learning tasks, and especially, the regression models. They avoid calls to external functions in the IAM so are faster in solving the problem. In addition, the weights or coefficients in the equations may be pedagogical when interpreting which flexibility options influence more or further integrate the VRES generation into the system (deeper decarbonization). The main contribution of this work is therefore to test a new fast and straightforward method for the IAM field.

To balance the compromise between accuracy and computational cost, as well as to take advantage of the available data, we have selected the hourly EnergyPLAN model [40] to represent the EU-27 region as a case study. EnergyPLAN is described in detail by H. Lund et al. in [41]. The trajectory of this model to analyze energy systems and propose indicators to assess at different levels – energy, economy, finances – of the energy transition has been recorded in the review written by P.A. Østergaard [42]. From the regression's point of view, a supporting feature of EnergyPLAN is the fact that this model only contains linear equations, so the method would already be enclosed into multiple regression models to reproduce the addition of several independent effects, e.g., the capacity expansion of solar and wind, or some flexibility options such as power-to-X technologies.

The structure of this paper is the following: first, the method is explained in detail (section 2). Next, the goodness of the method is shown in the results (section 3). Third, a discussion on the advantages and limitations of the research is carried out in section 4. Finally, some conclusions are written to summarize the key ideas and further work on this line of research in section 5.

2. METHODS

In this paper, the authors develop a method that should enable energy modelers to capture the interannual variability of VRES and the management of this variability through different flexibility options and represent them in IAMs, which usually have an annual temporal resolution. The method is based on the idea of using statistical indicators, such as the capacity factor (CF) of different technologies as a proxy for the hourly operation of a certain energy system. The temporal resolution of one hour is chosen, since, as discussed previously, it provides suitable granularity to study the operation of energy systems under different penetrations of VRES in the mix [43]. The developed method is comprised of four steps, which are graphically represented at the right of Figure 1.

In the first step, suitable input data for the energy system is gathered, so that it can be adequately modeled. Secondly, for that energy system, different possible future configurations are developed, by combining and mixing the shares of various supply and demand technologies. The specific process for generating the combinations of technologies is discussed later in the text. Once these configurations are developed, as a third step, the hourly operation of that energy system is simulated for each configuration, using an hourly time-step. At the end of each simulation, several numerical indicators are calculated to quantify the capacity factor of the different technologies. In a fourth step, the multiple linear regression analysis is performed, providing a relationship between the configuration of the energy system, on the one hand, and the values of the statistical indicators, which capture the inter-annual variability, on the other hand. The detail of the different steps in the method is described at the left of Figure 1.

When this method is used to generate relationships that can be used in an IAM, it should be ensured that all the technologies that are used as independent variables in the regression analysis should explicitly be represented in the IAM. In other words, care should be taken in order to ensure that the technical parameters of both models (the hourly-resolved and the annually-resolved model) are harmonized, to avoid inconsistencies.

In this paper, an input is a parameter in EnergyPLAN that is modified across combinations, while a constant is a parameter in EnergyPLAN whose value remains the same across combinations. A range is configured by the maximum and minimum values within an input can vary, so a point is a value within a range. A cluster is one input or a group of them that are modified simultaneously across combinations. Finally, a regression input is the combination of inputs selected to represent a cluster in the regression while an estimated output is the value of the cluster calculated from a regression model.

The next sections explain the inputs and outputs obtained with an hourly resolution, as well as the outputs selected to be regressed. The hourly-resolution model named EnergyPLAN is used in this work [44].

The reason for the selection of MLR models is twofold. On the one hand, a modeler can use different probability distributions depending on the bounds of the response (output). On the other hand, MLR models can be implemented into any model where other advanced tools such as those coming from machine learning theory cannot. Linear relationships have been considered for simplicity to test the method, safer than nonlinear shapes when the variables run out of ranges, a situation not recommended but considered as well for fine-tuning.

Supplementary materials consist of code and the data to reproduce the study. Such contents are well-structured in a Zenodo repository [45].

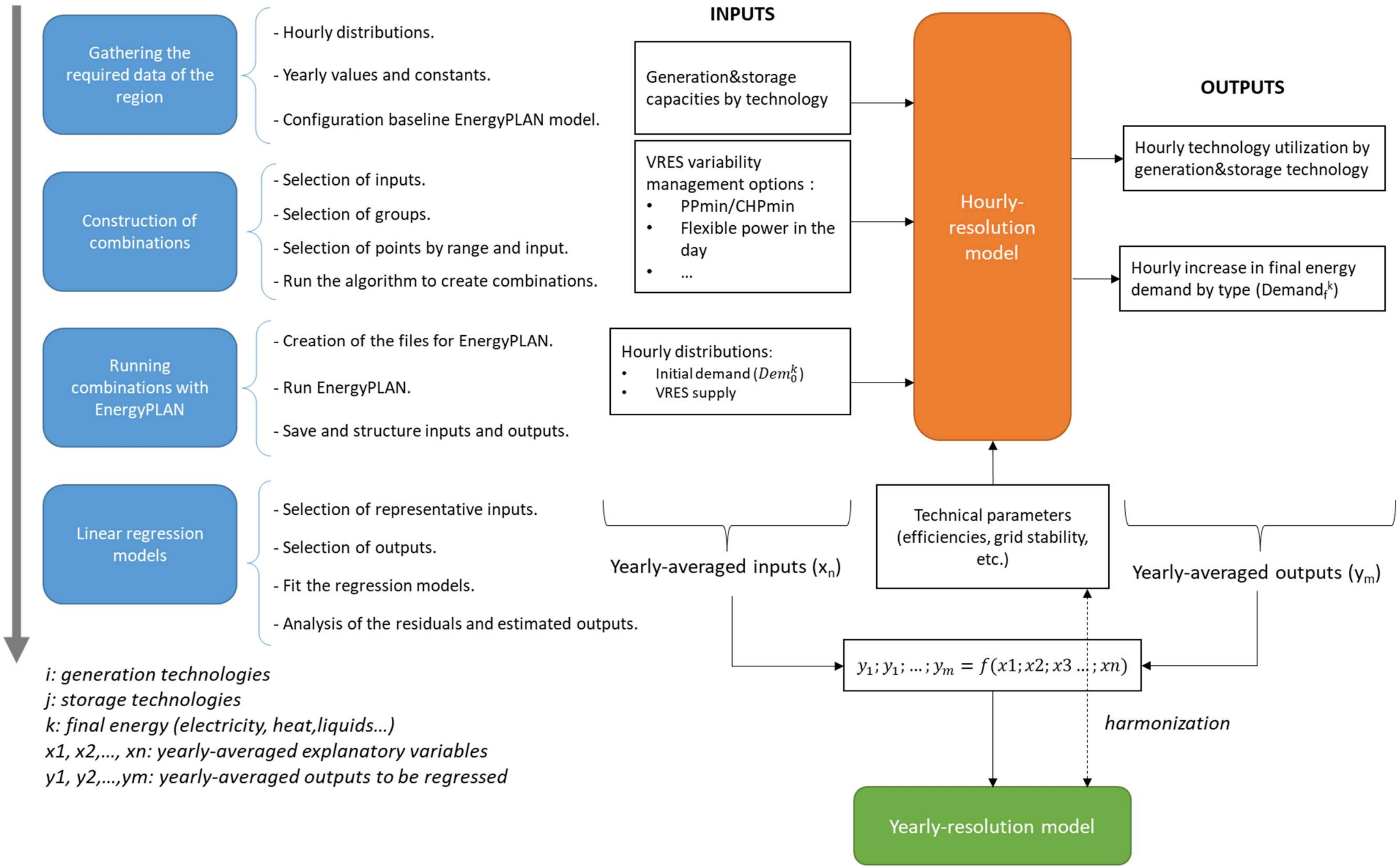

Figure 1. Overview of the developed approach (right) and steps and sub-routines of the method presented in this article (left). Own elaboration.

2.1. Design of the experiment

The objective of this article is to condense hourly information into annual input-output relationships. The introduction section supports that MLR models may be one option to do it, however, data is required to train and statistically prove this assumption.

The inputs and outputs of thousands of simulations with EnergyPLAN are the basis to fit the MLRs. The inputs represent technologies of interest – present in the energy model – that are going to be captured in the relational model. Thus, the selection of inputs and values per input are two crucial tasks that constitute what may be called the design of the experiment, i.e., an ad-hoc configuration of values to show variations in the outputs.

The configuration is created by combinations instead of permutations since the order does not matter, i.e., each input has some values or points that are unique, and they are not exchangeable with the values of the other inputs. Also, the resolution of inputs may differ according to the interest in the technology, e.g., later we will see that clusters of wind and solar have five points, but the cluster of storage has three. Behind the explanation, the objective focuses on variable renewable technologies as those causing risky variability.

Inputs from both the demand and supply sides are required to effectively represent the effect produced by the technology in EnergyPLAN. For instance, the role of power-to-heat (P2H) can briefly be explained as follows: this flexible option allows for using electricity to produce heat (electric boilers) or to move heat (heat pumps) in two complementary facilities, district grids, and the agents grouped as "individual" (not grid-connected). Consequently, the installed capacity of boilers and heat pumps, the fuel distribution for non-electric boilers, or the contribution of solar thermal are inputs of the supply side of the P2H option, while annual demands and hourly profiles of cooling and heating define the demand side of the option. Some simplifications are therefore addressed to avoid an excess of time when computing the combinations. This aspect is key in understanding the main limitation of the approach, i.e., the computationally feasible number of simulations. This limitation is explained in the next subsection.

The hourly profiles and other variables such as conversion factors and efficiencies are included as constants, given the great climate and meteorological uncertainty (IAMs deal with decades of analysis). Other variables such as the differences in efficiencies over time can be computed in post-processing adjustments within the IAM.

The application of EnergyPLAN for the objective of the research has been explained in a similar experiment where the structure of inputs is run in a multiple combination approach [46]. Such combinations are described by employing some features: name, range of values (maximum and minimum), and the number of values in the range (points of resolution). From a pre-defined condition, the scenarios achieving 100% renewable systems and intermediate situations at the hourly level are present in the data. The documentation of the version used in this study can be read in [44].

A Python script automatizes the process of creating input files, running EnergyPLAN, and saves outputs of interest for the MLR models. The clustering and pre-processing of data are done with MS Excel. Power Query software facilitates the creation of combinations as well as post-processing tasks with the results. Then, a Python code is used to run EnergyPLAN as many times as combinations are defined, translating the values of combinations into input files. Once the input files are generated, the energy model is run, and outputs are saved and properly allocated to the next steps of the method (MLR models). The entire code can be downloaded from the Zenodo repository.

Given the accessibility of data and the scale IAMs typically present, the EU-27 region as a whole has been considered to test the approach. The international interconnections of EU-27 with the rest of the world are neglected for the sake of simplicity (948 GW vs 41 GW; source: Eurostat, 2019). These connections are subject to conditions that fall out of the scope of this work like policy agreements between countries or how the other countries develop the energy transition, so this uncertainty is not captured. The values of constant parameters are shown in Table B. *3*.

While being aware that EnergyPLAN represents an energy system with a copper-plate equivalent and may not render the geographical resolution of large energy systems in detail; in this paper, it was used also due to the simplicity of its configuration and fast running procedures, which are key having in mind the number of simulations performed. These two factors combined to enable the fulfillment of the goal which is to obtain high-resolution data on the interactions between the capacities of variable renewables and flexibility options, and their influence on reaching the shares of renewable energy as well as their performance in the energy system. The level of detail lost during the aggregation of data is not insignificant but is the compromise that the modelers took to achieve the required results.

To automatize the ad-hoc configuration in EnergyPLAN, a distinction between the basic (or "legacy") electricity demand and the total electricity demand is made. The first one originated from the historical data and its projection. The second one includes the legacy demand plus all the new demands coming from flexible electricity demand (daily, weekly, and monthly), electricity for heat pumps, electric vehicles, and electrolyzers. In simulations, the basic electricity is then modified to stay at the same value in the total electricity demand.

2.2. Data collection

The hourly distributions of the electricity demands have been collected from ENTSO-E [47]. The distribution of heat demand has been calculated with the hour-degree method [48], which based the results on the temperature distributions and the operational characteristics of the district heating system.

Synthetic hourly profiles of VRES have been created with data from the *Renewablesninja* website [49]. The resulting curves are further calibrated with historical data to present a realistic energy mix. The database for the calibration process was IRENA [50]. All the distributions are available in the supplementary materials of this article (Zenodo's repository).

2.3. Combinations of inputs

The limitation aforementioned is mathematically rooted in combinatorial analysis. The time of computation can be approximated by the Equation 1, where t_s is the time spent in one cycle of running EnergyPLAN and saving the results, and p_c is the number of points in the cluster c (from cluster 1 to cluster n). The machine used for this work is the Acer Aspire V5 552 g with AMD A10 5757 M and 8 GB of 800 MHz memory. So, the code has been successful in bringing the average time required to perform a cycle to 1 second. Therefore, a maximum of 3600 cases would be run in one hour, 86400 in a full day, and so on. The time exponentially increases with the number of points and inputs.

$$t = t_s \cdot \prod_1^n p_c \qquad \text{Equation 1}$$

Once the limitation is on the table, the authors suggest grouping inputs in a clusterization based on what defines the technology represented. As consequence, all the inputs of EnergyPLAN involved in the same cluster are changed in unison with combinations. The full list of clusters with their definitions is shown in Table B. *1*, in which values are placed in Table B. *2*. The condition of modeling a wide range of energy systems, from 100% fossil-fuel-based to 100% renewable-based continues to be satisfied. The decarbonization of an energy system can be achieved in numerous ways. The capacities of flexibility options are then selected to enable this possibility and our estimations are described in the last column of Table B. *1*.

The clusters reflect when different technologies have a similar application. This is the case with stationary batteries, pumped hydropower, and rock-bed energy storage. All these technologies are similarly reproduced in EnergyPLAN, disagreeing in the available capacities, round-trip efficiencies, and economics, but not the way they operate in the system. So, given the reference scenario parameters, results can be split into different technologies (post-processing).

Two criteria are followed to set up the ranges of values. First, to achieve patterns of capacity factors related to the flexibility implemented in the system. It is useful to assess the best options in the region. Second, the scenarios of carbon-neutral and 100 % renewable energy systems are included to cover all the transition options.

To achieve both, the capacities of VRES technologies have to be significantly increased in comparison to the current situation. The range of wind onshore goes from 0.5 to 2.5 TW (around 50% of the projected potential for onshore wind energy in EU-27 [51]), but the potential capacity is highly dependable on land-use restrictions. On the other hand, the installation of offshore wind farms has a range from 0.08 and 3.8 TW, while the range for simulations goes from 0.05 to 0.25 TW. Finally, the potential for solar-PV capacity is within the range of 0 - 1.2 TW when it only considers the investments for installations on rooftops and the brown field. This potential is smaller than the maximum (2.5 TW), but the investments into new projects on unused land should also be considered [52].

EnergyPLAN's warnings[†] are saved to decide whether repeat the combinations or not. Thus, the results must finally be manually checked to ensure that errors do not arise.

Some additional general ideas should be considered at this step:

[†] EnergyPLAN might deliver some warnings after the simulation is run: critical excess of electricity production (CEEP), grid stability problem, power plant or import problem, synthetic or biogas shortage, V2G connection too small, and negative electricity demand. Further information in the documentation of EnergyPLAN.

- Inputs of EnergyPLAN can be sorted into first, second, and third spheres of influence when defining a technology. Then, the modeler can select more or less inputs to define the cluster according to the resolution looked for in the analysis of that technology.

- Projections help to determine what variables should have a wider range to better consider their flexibility effects. The information on what should be considered constant also came from the projections.

It is here emphasized that clusters have fixed ranges to perform the combinations, so the results are correct as long as the model does work within the extreme values of the ranges. Beyond them, the reliability of results is not guaranteed but the MLR models are robust (linear) so the error included could not be as extreme as the one committed by a nonlinear function.

A total of 174960 simulations were run by a combination of 8 clusters (39 inputs, Table B. *2*).

2.4. Multiple linear regression (MLR) models

The results that are of significant value for further advances in implementing variability effects into IAMs are the ones that represent the relationships between the level of technology implementation and the resulting change in the capacity factor and demand.

The data collection gathered from the previous step, i.e., the process to generate combinations between the inputs, is used to represent each output through multiple linear regression models. Additionally, the inputs and outputs from combinations have been adapted for the type of probabilistic distribution fitting the models (logistic). The regression inputs (independent variables) can be shown in Table 1. They are normalized between 0 and 1 to avoid scale effects that usually cause disbalance in the weights of the regression terms. On the other hand, the outputs (dependent variables) are shown in Table 2, in which values are constrained between zero and one. PHS means pumped hydropower storage; CHP means combined heat and power; PP means thermal power plants; and HP means heat pumps. Finally, the options to provide flexibility in the system are linked to the capacities of variable renewables, as the back-up units are to the installed capacity of the whole park.

The reason behind the selection of logistic distributions for most of the outputs is the fact that the inputs are discrete by design in the experiment (2, 3, 4 points in the range), and not continuous variables (e.g., ranges based on uniform distributions). Consequently, the response (output) can be assumed to follow a binomial probability distribution. Two exceptions have been considered, the demand for electricity and the generation of natural gas (available synthetic gas), which are also effects caused by the different configurations in the mix, so captured in the regression models. These two variables are not limited between 0 and 1, so a normal distribution fits the model, instead of a logistic one.

A realistic maximum for each capacity factor (CF) has been assumed by technology, to compute the relative variation of the output (Table 2, second column).

Table 1. The regression inputs and outputs are considered. SynthGas to synthetic gas produced with hydrogen. Grid stability is defined between 0 and 1 in EnergyPLAN. Name definitions are explained in Table B. 2.

Regression input name	**Regression input definition (as a function of combinations' inputs) [dimensionless]**
$wind$	$\frac{wind\ onshore\ capacity\ [MW] + wind\ offshore\ capacity\ [MW]}{total\ capacity\ [MW]}$
$solar$	$\frac{solar\ PV\ capacity\ [MW] + solar\ CSP\ capacity\ [MW]}{total\ capacity\ [MW]}$
$geothermal$	$\frac{geothermal\ capacity}{total\ capacity\ [MW]}$
Baseload	$\frac{PP\ minimum\ [MW] + CHP\ minimum\ [MW]}{total\ capacity\ [MW]}$
DSM	$\frac{flexible\ power\ in\ the\ day\ [MW]}{total\ VRES\ capacity\ [MW]}$
$ElecTransport$	$\frac{smart\ EV\ charging\&discharging\ \ [MW]}{total\ VRES\ capacity\ [MW]}$
$P2H$	$\frac{P2H\ capacity\ [MW]}{total\ VRES\ capacity\ [MW]}$
$Storage$	$\frac{grid\ batteries\ [MW] + PHS\ [MW] + rockbed\ storage\ [MW]}{total\ VRES\ capacity\ [MW]}$
$FossilIndustry$	$\frac{natural\ gas\ in\ industry[TWh]}{total\ demand\ in\ industry\ [TWh]}$
$SynthGas$	$\frac{production\ of\ synthetic\ gas\ [MWh]}{total\ VRES\ capacity\ [MW] * 8760\ [h]}$
$GridStability$	$Grid\ stability[dmnl]$

Table 2. Nomenclature and definition for the outputs of interest. *VarElecDemand* and *VarNatGas* mean variation of the electricity demand and natural gas, respectively (related to the reference configuration values).

Regression output name	**Max CF of the technology (%)**	**Regression output definition (as a function of results from EnergyPLAN) [dimensionless]**
$VarCFwindOn$	23.2	$\frac{\max(CF_{windOn}) - CF_{windOn}[TWh]}{\max(CF_{windOn})\ [TWh]}$
$VarCFwindOff$	36.8	$\frac{\max\left(CF_{windOff}\right) - CF_{windOff}[TWh]}{\max\left(CF_{windOff}\right)\ [TWh]}$
$VarCFsolarPV$	12.1	$\frac{\max(CF_{solarPV}) - CF_{solarPV}[TWh]}{\max(CF_{solarPV})\ [TWh]}$
$VarCFchp$	64.5	$\frac{\max(CF_{CHP}) - CF_{CHP}[TWh]}{\max(CF_{CHP})\ [TWh]}$

$VarCFnuclear$	89.3	$\frac{\max(CF_{nuclear}) - CF_{nuclear}[TWh]}{\max(CF_{nuclear})\ [TWh]}$
$VarCFpp$	93.6	$\frac{\max(CF_{PP}) - CF_{PP}[TWh]}{\max(CF_{PP})\ [TWh]}$
$VarCFhp$	62.4	$\frac{\max(CF_{HP}) - CF_{HP}[TWh]}{\max(CF_{HP})\ [TWh]}$
$VarElecDemand$	-	$\frac{Electricity\ demand[TWh]}{Base\ electricity\ demand\ \ [TWh]}$
$VarNatGas$	-	$\frac{Natural\ gas\ consumption\ [TWh]}{Base\ natural\ gas\ consuption\ \ [TWh]}$

After the data is imported, the process can be sorted into three steps.

First, multiplicative terms (a couple of inputs without repetition) are calculated to add nonlinear effects to the list of inputs. Second, the selection of independent variables is carried out through the correlation coefficient, as many variables with the highest score loop up to a score below 0.05. This implicitly assumes that there is no more information to be gotten from the data. Third, the list with the selected variables performs an MLR model based on either a binomial or normal probability distribution by output, according to the output (aforementioned). Finally, the results are automatically printed to compare the actual values calculated by EnergyPLAN and the ones by the MLR models. The fitting of goodness for each MLR model is assessed through general statistics such as the R-squared adjusted or the p-value of hypothesis tests, and others like the analysis of outliers, slice plots, and visual comparison.

The code is saved in an open-access Zenodo repository [45].

3. RESULTS

The first part of this section presents the combinations in terms of flexibility options and renewable penetration in the system. The second one is the statistical analysis of the MLR models.

3.1. Combinations in EnergyPLAN

In the present article, the focus is on the statistical analysis of data generated with an hourly energy model. Data comes from a previously published work where the requirements of several flexibility options are computed for the integration of large renewable shares, and energy transitions towards 100% renewable and integrated energy systems (Pfeifer et al 2021 [46]). The results of the present article aim to improve the treatment of renewable energy generation from variable sources.

The EnergyPLAN simulations are presented in annual values, which come from performing calculations at an hourly level. For that purpose, the relationship between the capacity factor of onshore wind, and the share of renewables in primary energy is displayed as an example in Figure 2. Some comments are included to show the influence of the flexibility options at different levels (in brackets), as well as the influence of different capacity levels of renewables. A zero ("0") represents those cases in which the technology was not used, while one ("1") represents cases with complete use of it. The first three values are related to the used capacities of wind, photovoltaic, and geothermal power capacities. The remainder is defined by order to the thermal power plant flexibility, transport electrification, power-to-heat, demand-side management, industry decarbonization, grid operation requirements, and the generation of synthetic gas.

As expected, the cases with the highest flexible capacity in the system are such that achieve the highest renewable shares, so the highest capacity factors as well. It may be noted that the results marked with the same color correspond to the same system configuration of flexibility options. Besides, the capacities of renewables play a major role. Due to the uniformity of these inputs across the combinations, there are cases in which significant problems to employ the available energy. When the capacity to generate is available, but the demand is lower (lack of flexibility options), curtailment will arise to match both sides.

Figure 2 shows the capacity factor of wind onshore in terms of the renewable share in the system. All the combinations are represented, where some sets are highlighted as examples to explain the figure. The green and red combinations are configured with the same level of renewable installed capacity; however, the flexibility options in the green set are significantly greater. Consequently, the CF in the green case is higher – so power units are more used – than in the red case. Additionally, another two sets (magenta and blue) are represented to show differences in the vertical direction. In these cases, the flexibility options are the same and the renewable capacities are not (higher for the blue case). Despite having similar renewable shares, the magenta case results are much more optimal (managing a higher CF) than its blue equivalent. The depletion in the CF is therefore sharply when the flexibility options cannot absorb the overproduction coming from the variable renewable generations. It is concluded the role of *new* electricity demand to remain the capacity factors high.

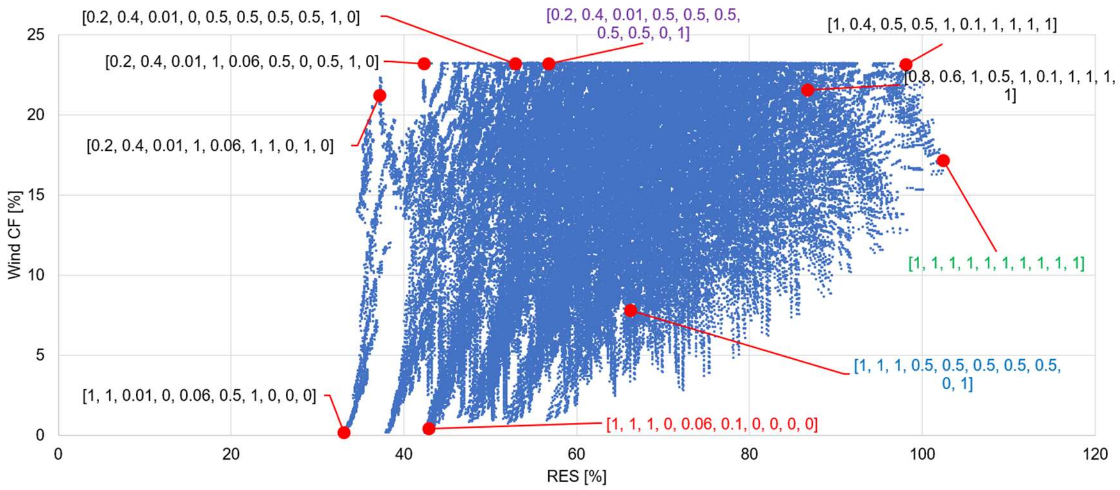

Figure 2. Flexibility vector on the results for the capacity factor of onshore wind in EU-27 region.

Further clarification of the results and the influence of flexibility options are visible in Figure 3 (same example with the onshore wind technology). A window of the data contained in Figure 2 is here enlarged. The lines correspond to constant configurations of flexibility options to show which of them can integrate more VRES capacity, i.e., the lines staying at the top more rates of renewable penetration. The orange line (right) has all the options equal to one, while the blue (left) presents zeros.

The results of these simulations reflect a positive increment in the electricity demand, due to the increasing role of the electricity in the energy system (heating, e-mobility, hydrogen), efficiencies, and energy conversions.

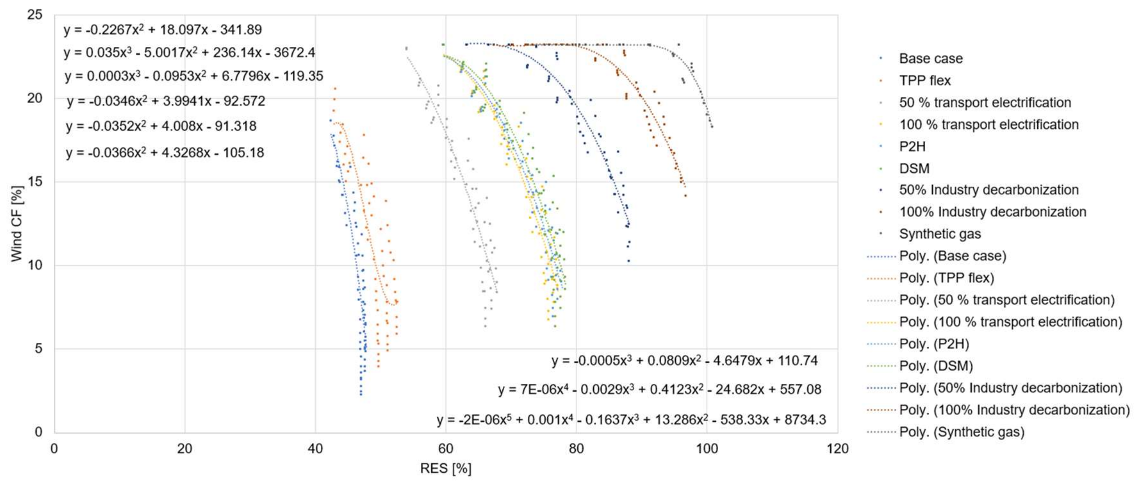

Figure 3. Selected curves represent one possibility of flexibility integration progression.

3.2. MLR models

General statistics for all the outputs of interest were summarized from Figure 4 to Figure 12. Despite all the regression models being statistically significant (p-value practically equal to zero), the accuracy in representing the outputs varies from quite well-fitting such as *VarCFwindOn* (0.90) to the worst for *VarCFnuclear* (0.59). This aspect allowed us to discuss possible reasons for the differences (next section). We have used the first output (*VarCFwindOn*) to explain the remainder of this section.

Figures 4-12 show the correlation between the same output with EnergyPLAN and the MLR model. The cloud of dots falls close to the red line, which reproduces the hypothetical perfect regression. Nuclear presented two different patterns, one “S” shape (logistic type) with 55% of flexibility (CF between 0.45 to 1) and another dot pattern with 100% flexibility (CF between 0 and 1) like the output *VarCFpp*.

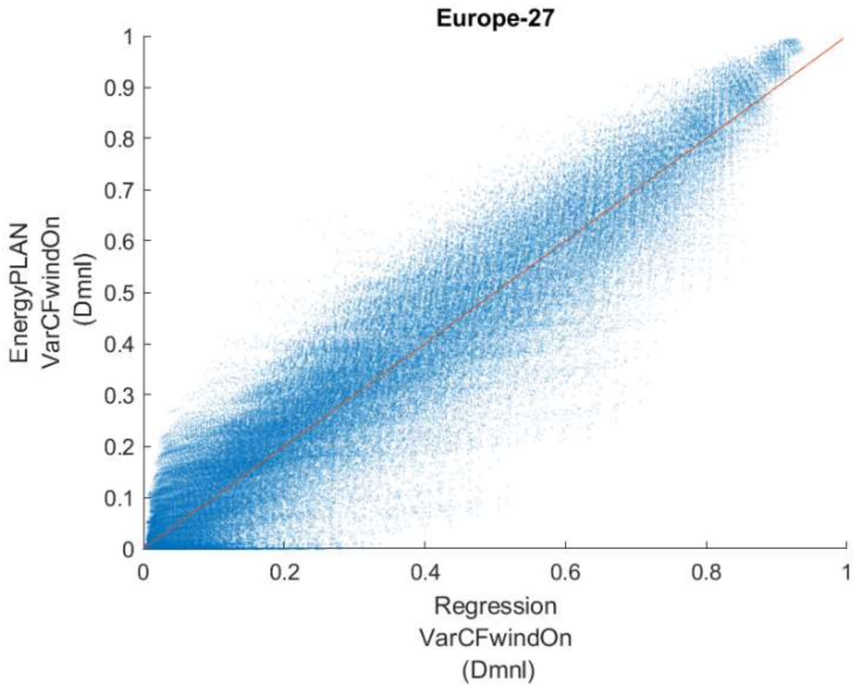

Figure 4. Estimated output of VarCFwindOn in the EnergyPLAN’s results compared to the results of the regression model. R-squared adjusted: 0.9023; p-value: 0.0000. Probabilistic distribution function: Binomial.

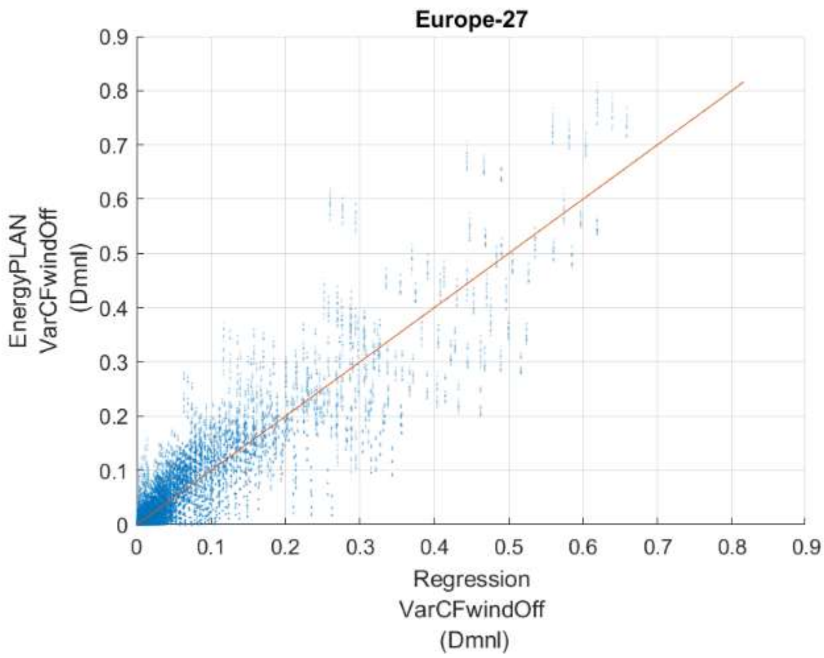

Figure 5. Estimated output of VarCFwindOn in the EnergyPLAN's results compared to the results of the regression model. R-squared adjusted: 0.8538; p-value: 0.0000. Probabilistic distribution function: Binomial.

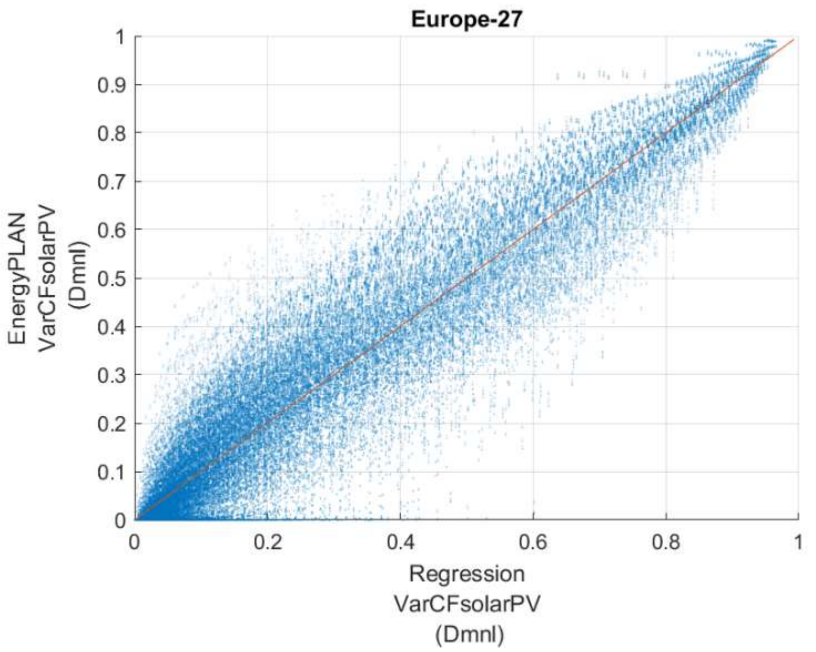

Figure 6. Estimated output of VarCFwindOn in the EnergyPLAN's results compared to the results of the regression model. R-squared adjusted: 0.8995; p-value: 0.0000. Probabilistic distribution function: Binomial.

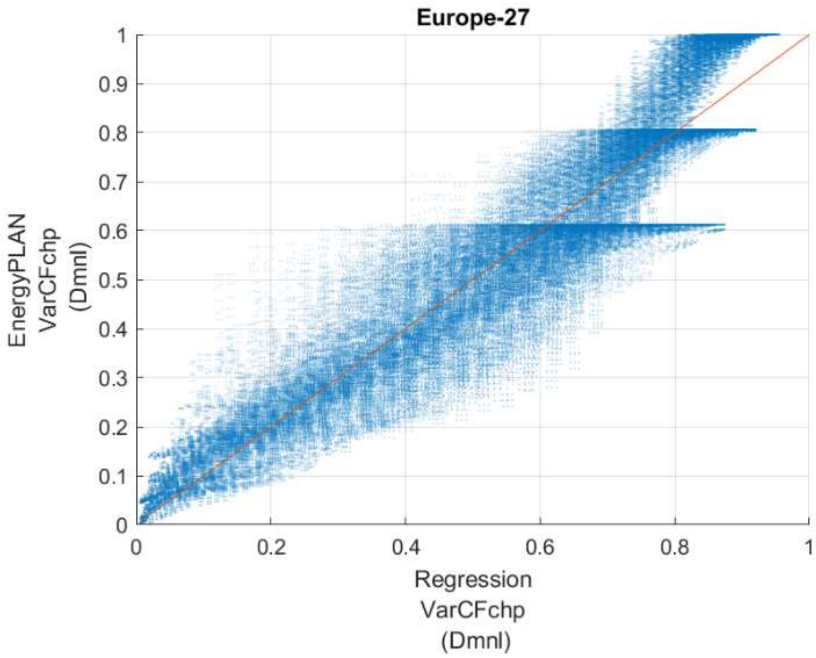

Figure 7. Estimated output of VarCFwindOn in the EnergyPLAN's results compared to the results of the regression model. R-squared adjusted: 0.8786; p-value: 0.0000. Probabilistic distribution function: Binomial.

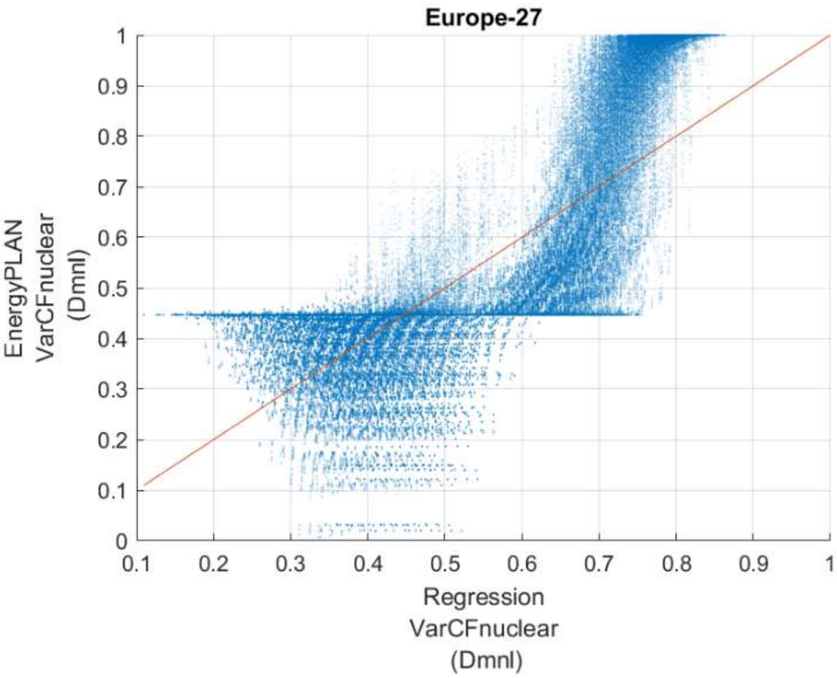

Figure 8. Estimated output of VarCFwindOn in the EnergyPLAN's results compared to the results of the regression model. R-squared adjusted: 0.5867; p-value: 0.0000. Probabilistic distribution function: Binomial.

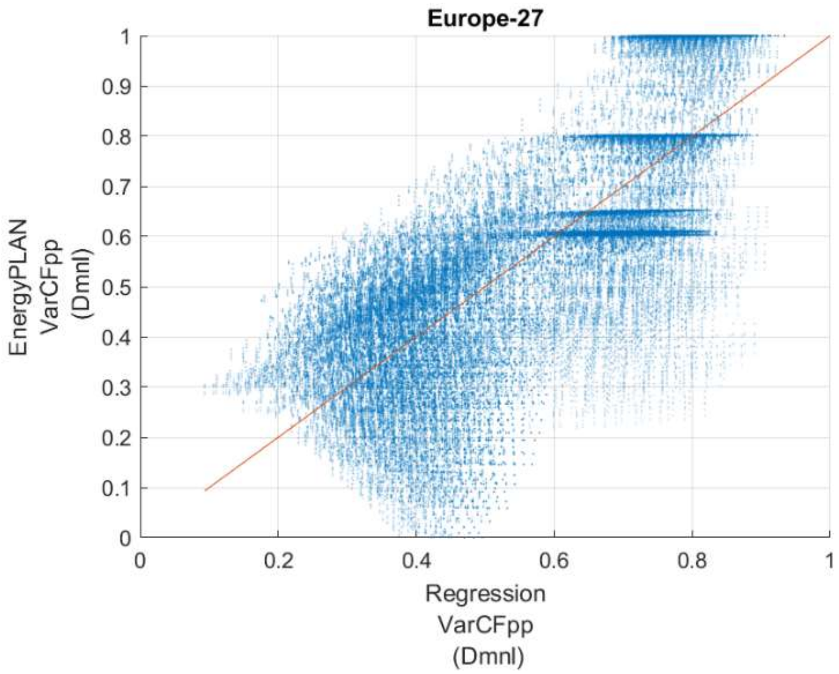

Figure 9. Estimated output of VarCFwindOn in the EnergyPLAN's results compared to the results of the regression model. R-squared adjusted: 0.6121; p-value: 0.0000. Probabilistic distribution function: Binomial.

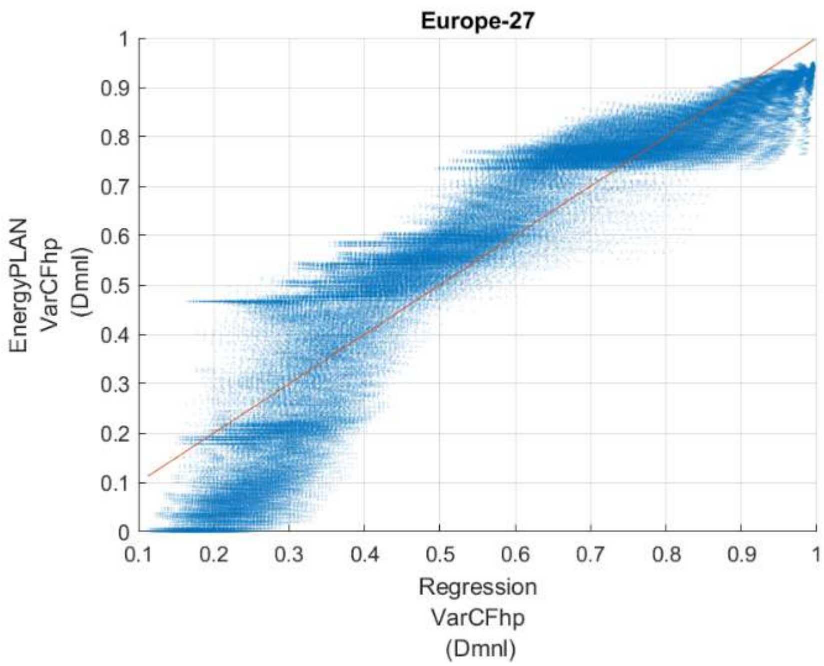

Figure 10. Estimated output of VarCFwindOn in the EnergyPLAN's results compared to the results of the regression model. R-squared adjusted: 0.8615; p-value: 0.0000. Probabilistic distribution function: Binomial.

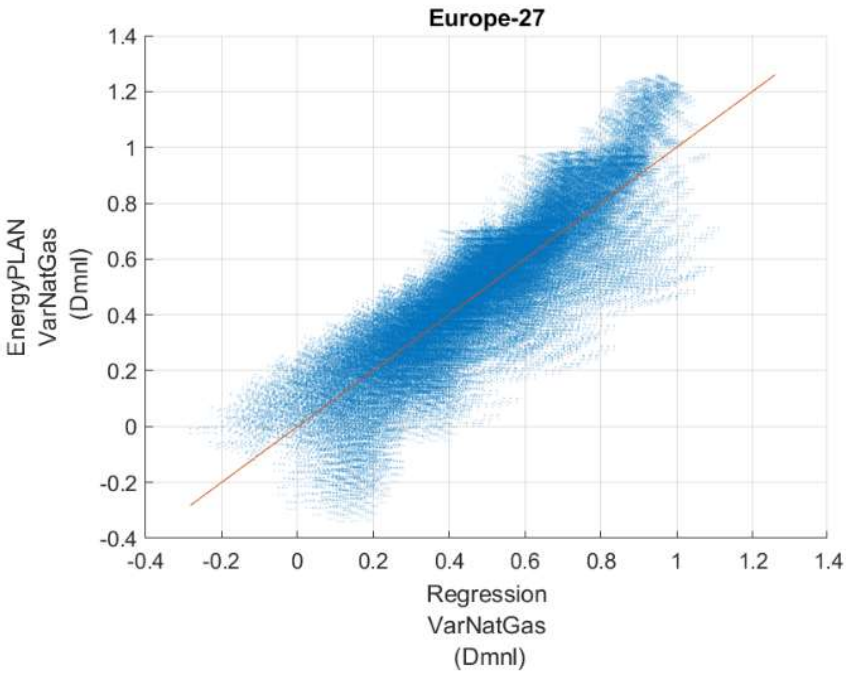

Figure 11. Estimated output of VarCFwindOn in the EnergyPLAN's results compared to the results of the regression model. R-squared adjusted: 0.7481; p-value: 0.0000. Probabilistic distribution function: Normal.

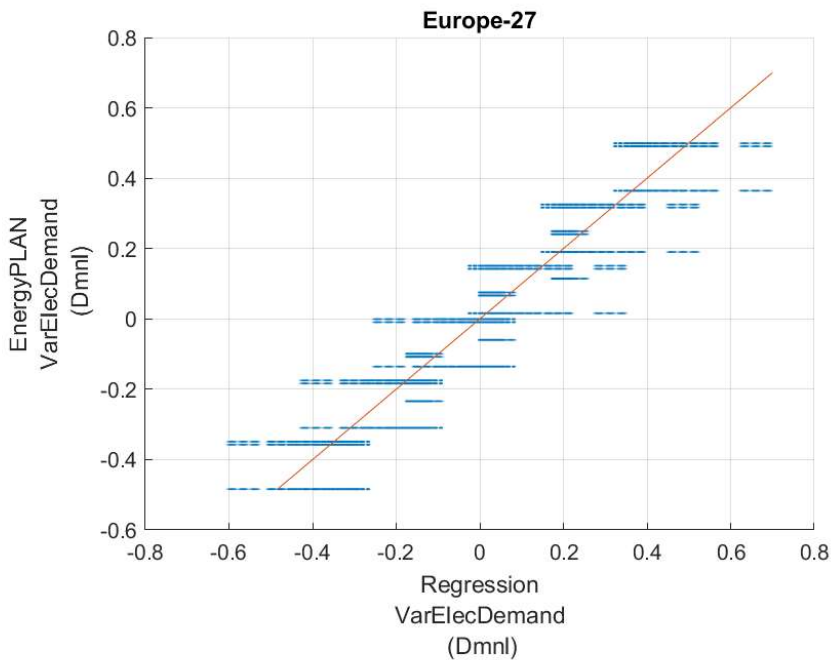

Figure 12. Estimated output of VarCFwindOn in the EnergyPLAN's results compared to the results of the regression model. R-squared adjusted: 0.8764; p-value: 0.0000. Probabilistic distribution function: Normal.

VarCFwindOn has been used as an example to explain the next results. The other outputs are included appendices. Table 3 represents the loop iterations results for *VarCFwindOn*. We can see correlation coefficients always above the criteria (0.05), and how much information (R-squared) was captured by each of the regression inputs. The nonlinear multiplicative term between *wind* and *solar* clusters (*Wind_Solar*, i.e., *wind* • *solar*) seems to be highly correlated, representing about 23% of the information in the equation (normalized R-square adjusted values). It is selected in an iteration when the nonlinear relationship delivered the highest correlation factor (>0.05). On the other hand, the repetitive terms mean that the cluster can include more information about the output of interest. Computationally, they come from the same reasoning as Wind_Solar, i.e., the highest correlation factor was achieved by Storage in iterations 6 and 11 when selecting the inputs for *VarCFwindOn*. The rest of these tables were saved in APPENDIX C. Number of inputs differs from one output to another. Thereby, *VarCFchp* (0.88, Figure 7) iterated 15 times while *VarCFwindOff* (0.85) did it 7 times.

Table 3. Inputs selected over iterations to build the regression model for the output *VarCFwindOn*. Combined inputs (input 1 * input 2) are represented by '_'. A correlation coefficient of 0.05 was the criteria to stop the loop.

Regression input	Correlation coefficient	R-squared adjusted
Wind_Solar	0.53	0.28
FossilIndustry	0.48	0.23
SynthGas	0.44	0.19
GridStability	0.34	0.12
ElecTransport	0.34	0.12
Storage	0.23	0.05
Wind_Solar	0.30	0.09
Wind	0.28	0.08
Geothermal	0.20	0.04
Wind_Solar	0.12	0.02
Storage	0.11	0.01
Wind	0.09	0.01
Wind_Solar	0.09	0.01
P2H	0.09	0.01
DSM	0.06	0.00

Cook's distance (D_i, Equation 2) is useful for identifying outliers longer than a threshold (three times the mean of Cook's distance as rule) It is calculated by removing the ith combination from the model and recalculating the regression. $\widehat{Y_{J(\iota)}}$ is the fitted response value when excluding *i*. *MSE* is the mean squared error of the regression model. *p* is the number of predictors. A plot of this indicator for *VarCFwindOn* is shown in Figure 13 (to see more, APPENDIX G). In the case analyzed, we can see several highly influential combinations upper the threshold (dotted line), which involves 8.42% of the combinations. *VarCFsolarPV* accounted the highest percentage of outliers (8.48%) while *VarCFnuclear* the lowest (5.86%).

Equation 2

$$D_i = \frac{\sum_{j=1}^{n}(\hat{Y}_j - \widehat{Y_{j(i)}})^2}{p \cdot MSE}$$

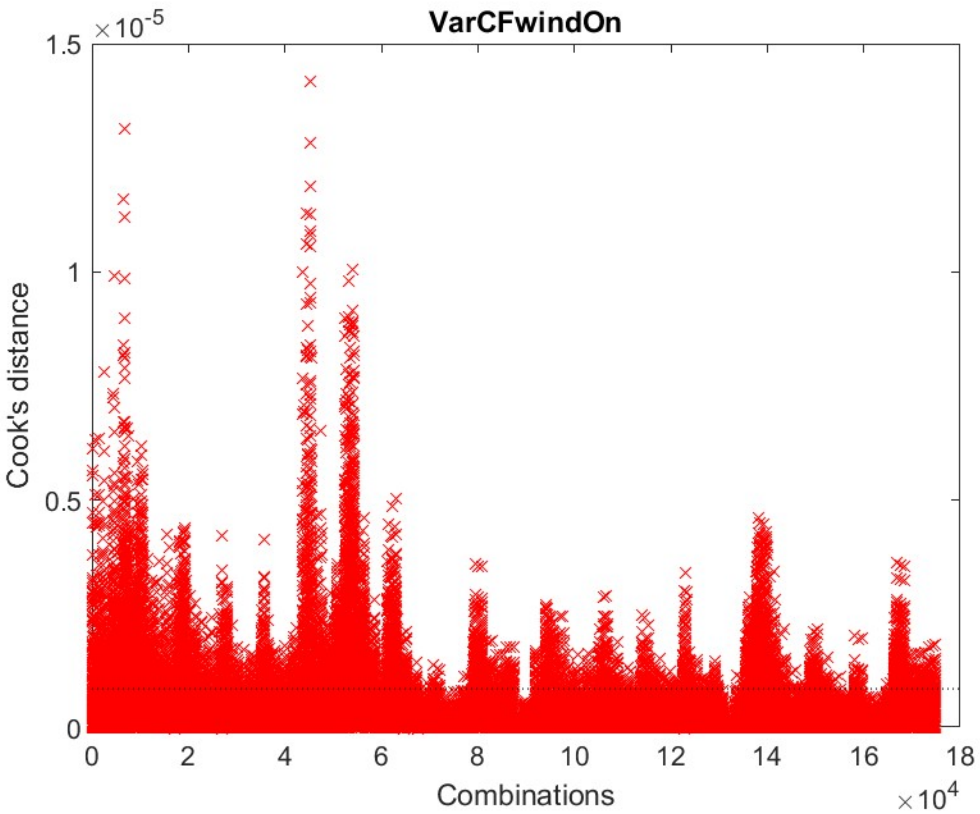

Figure 13. Plot observation diagnostics of outliers (Cook's distance) MLR model for "VarCFwindOn". The dotted line represents the recommended threshold value of three times the mean.

Inference about coefficients of regressions is carried out through hypothesis tests in t-statistics. Table 4 shows the t-statistic (*tStat*) and related p-value by regression input (row). Every p-value fell low, so coefficients were statistically significant. If we look at similar tables in APPENDIX E all the p-values were below 0.05, usually, the criteria to consider the null hypothesis true. We may conclude that selection of features based on the correlation coefficient is validated.

Table 4. Hypothesis test on t-statistics for the output *VarCFwindOn*. 5% of significant level. *SE*: standard error of coefficients. *tStat*: t-statistic.

Regression input	SE	tStat	p-value
DSM	0.58	-12.39	2.97e-35
ElecTransport	0.02	-67.70	0
FossilIndustry	0.02	105.74	0
Geothermal	0.66	23.08	7.29e-118
GridStability	0.04	62.60	0
P2H	0.59	-16.20	4.82e-59
Storage	0.22	-56.53	0
SynthGas	0.42	-89.95	0
Wind	0.06	63.67	0
Wind_Solar	0.32	45.10	0

Finally, slice plots show the regression surface predicted, i.e., the fitted response values as a function of a single predictor variable (green line) with the other predictor variables held constant. 95% confidence bounds are also displayed in top and bottom dot red lines. Predictors remained within narrow response surfaces. For instance (Figure 14), when *ElecTransport* was equal to 0.10366, *VarCFwindOn* was estimated in 0.037599 [0.0328705, 0.0429779], an 16% of uncertainty with 95% of confidence (more figures in APPENDIX F). These figures visually provided a rational behavior between the regression input and the output, e.g., a positive relation between *Wind_Solar* and *VarCFwindOn* meaning that the higher is the installed capacity of renewables in the system, the higher is the loss of electricity in such generation units, for the rest of the system remains constant. Another example is the negative relation between *ElectTransport* and this output has coherence in the way that more V2G capacity implies more flexibility to allocate curtailment, so less variation in the capacity factor respected to the maximum of the technology. The slope is indicative of the estimator regarding the general stability of the output in the power system. *SynthGas* of *FossilIndustry* presented high slopes in their slice plots, thus, they strongly affected the output.

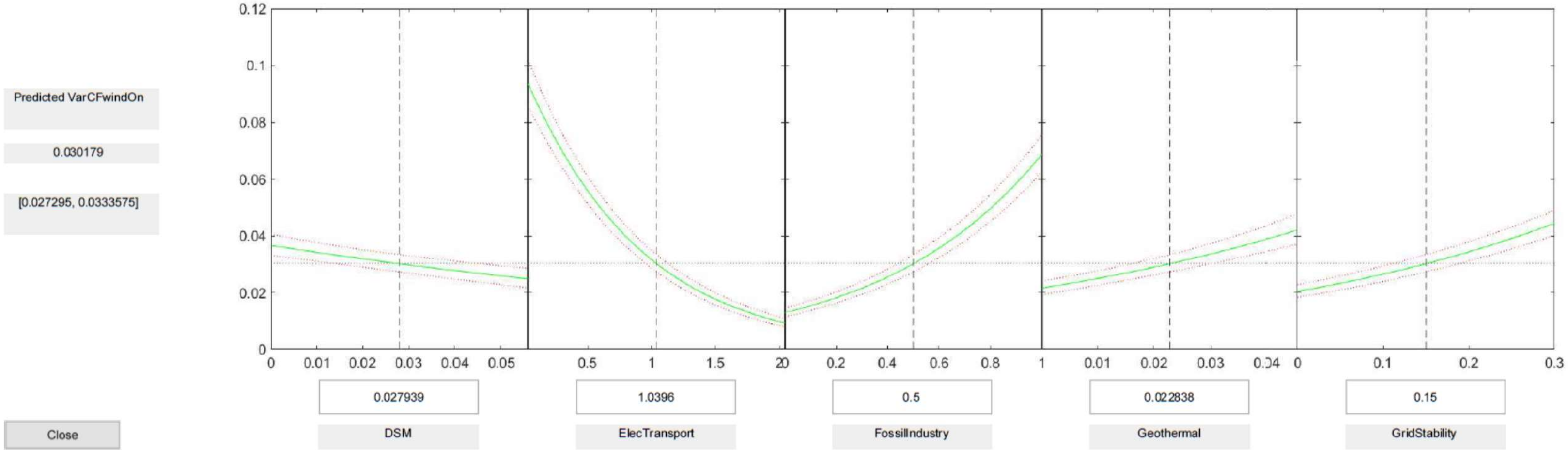

Figure 14. Slice plots of some regression inputs for the output 'VarCFwindOn'. Units: dmnl.

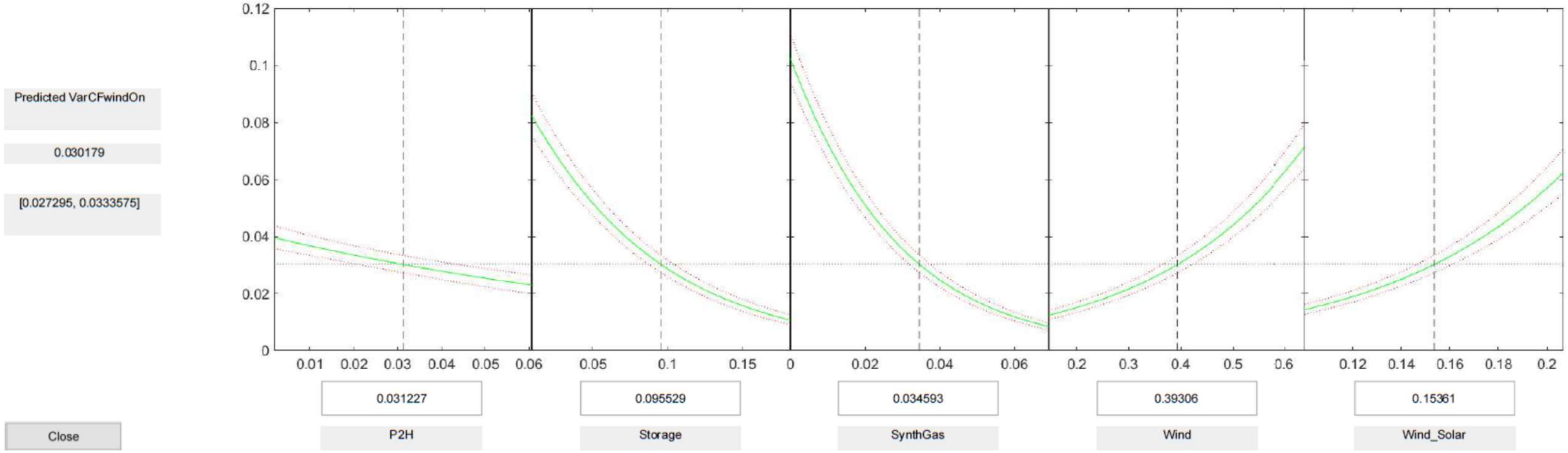

Figure 5 (continued)

4. DISCUSSION

Different methods to represent sub-annual information in IAMs have been reviewed in the literature review of the introduction section. At least, a time resolution of 8 hours has been found to achieve an accurate representation of the fundamental effects caused by the variable renewable generation in the energy system of models. The group of methods called representative time windows (time slices) is becoming obsolete in comparison with the hourly and sub-hourly analysis. This work contributes to the IAM field with a stylized approach based on 1-hour resolution and multiple linear regression models. However, similarly to the RLDC approach, the dynamics over consecutive hours are lost in the developed method. EnergyPLAN captures the hourly dynamics, but the MLR models implicitly save this information from the results of combinations.

The clustering step is considered a sensitive task of the process. The expertise in the energy model to be used in the approach (EnergyPLAN in this work) is required to identify which inputs should be selected and group them into representative technologies and specific coherent values to perform the combinations.

The MLR models fit reasonably well for most of the outputs. Nonetheless, two exceptions have been highlighted, *VarCFpp* and *VarCFnuclear*. The loss of accuracy in the regressions may arise from three reasons. First, the cluster is not correctly represented, i.e., more inputs are required in EnergyPLAN to better render the effect produced by the technology. Second, the existence of non-linearities so a poor representation when fitting the linear regression models. Third, the cluster requires a greater number of points to represent the range of values.

The number of combinations is a bottleneck for introducing more information about the system. The computational cost to perform the combinations has been the week (roughly), a duration that exponentially increases with new points and clusters (equation 1).

Going into details of the code to generate the MLR, in general, the algorithm assures the convergence to the criteria (Pearson's coefficient equal to 0.05) to deliver a set of statistically correlated inputs for the MLR model, while correctly choosing the best probability distribution to fit the model.

All the inputs selected for the MLR models have shown a p-value below 5% in the Student's tests, so statistically significant. The inputs are coherent with the equations of EnergyPLAN (Table C. *1*). For example, *VarCFwindOn* does not rely on the installed capacity of solar power plants, and vice versa; while *VarCFchp* relies on the grid stability share. The positive values correctly reflect the penalty in the capacity factor of these technologies. The higher the wind capacity, the lower the CF of this technology will be (remaining the rest constant). Another example is that synthetic gas is flexible in decarbonizing the system while reducing the CEEP, so the approach has shown the significance of this fuel along with all the outputs. The effect is visible with a negative term in *VarCFwindOn* and *VarCFsolarPV* outputs, and a positive term for the variation of natural gas consumption (*VarNatGas*). It implies that the higher is this input, the higher the VRES generation and consumption of gas will be. Finally, the results show a negligible penalty to the wind offshore technology (*VarWindOff)* so barely influenced by the curtailment. This is derived from the CEEP strategy, where both solar-PV and onshore wind has been considered for the curtailment measure but not the offshore wind technologies.

The presence of nonlinear terms in MLR models cheers up the discussion on whether the nonlinearity should be studied. *Wind_Geothermal* (and not *Geothermal*) is present in only one output, *VarNatGas*. On the one hand, these terms are generated from the combination of inputs, which may compete with the original ones. If so, the method could be introducing collinearity and correlation terms that don't introduce additional information in the analysis. On the other hand, the slice plots show narrow nonlinear bands (*VarCFwindOn*), a positive aspect supporting a conclusion made years ago by Alan L. [53], who stated that the nonlinearity *"should be limited to experimental studies"*, like the one we have carried out in this work. In summary, a deeper insight could clarify the role and shape of nonlinear terms in MLR models.

The configurations have covered a wide range of values per technology. Some of them run with almost nothing generation from VRES, while others do it with high shares. Although most of the Cook's distances have fallen below the limit, a remarkable number of combinations did it upper the bound. This is problematic since those combinations are not appropriately captured by the MLR model. Most outliers are derived from configurations with low shares of inflexible units (*Baseload* and *GridStability*) and high or very high shares of VRES.

The exercise has demonstrated the relevance of the experiment design. The output *VarCFnuclear* presents a two-level pattern, similar to the stepped dot cloud in *VarCFpp*. The cause behind these bad regressions is rooted in the variation of some parameters that should be constant assumptions, e.g., the nuclear part load (*Baseload* cluster) and the minimum grid stability (*GridStability* cluster) parameters. They behave as "if then else" switches in EnergyPLAN, so several combinations fall at the same horizontal threshold (around 0.45 in *VarCFnuclear*). However, other outputs show a more spread pattern so less influenced by the assumption, that is the case of *VarNatGas*. It is therefore highlighted that dispatchable thermal power plants (PP2) and nuclear units are both in the last positions of the power supply, i.e., the implicit information about these technologies in the combinations data is the most complex to be captured so their MLR models require more inputs to capture more relationships of EnergyPLAN.

Despite EnergyPLAN has been used for this work, the method is sufficiently general that it could, in principle, be applied to any couple of hourly and annual-resolution models due to its heuristic nature and fast calculation time. Once the MLR models are fitted, they provide, through input-output thinking, feedback on the behavior (CFs) of the technologies involved in the model.

A visualization of the cross-comparison of different criteria between the developed approach and the rest of the aforementioned methods has been included in Table 5. The next points discuss ideas from it:

1) The dynamics over consecutive hours are normally captured by the energy models, but these dynamics over the whole year are lost in time slices and duration curves [54]. This will inevitably lead to issues when checking the hourly (and sub-hourly) reliability of the power system. Furthermore, when providing flexibility options, there is no way to implicitly account for the power ramps of the technologies, an effect that such methodologies do not capture. This work, however, could capture the power ramps whether the energy model consider them, which was not the case with EnergyPLAN.

2) The uncertainty analysis of the parameters present in the modeling of the power sector is growing up in the literature about IAMs [55], and this work opens a new avenue in this matter. Although the values of the inputs are set up by combinations, uniform, triangular, or normal probability distributions could be designed to set up those values and effectively generate a confidence interval per parameter. The sensitivity analysis (e.g., Montecarlo) usually employs these intervals to deliver a range of possible scenarios and better assess the policies tested in the IAM.
3) The authors agree with Ueckerdt et al. [56] on the limitations of collecting the regional-specific data. This work assumes constant hourly profiles for both demand and supply sides, a source of uncertainty subjected to changes in climate phenomena and consumption patterns in our society.

Table 5. Summary of features for different methods, including the developed approach of this work.

Methods/ Criteria	**Time slices**	**RLDC (time-aggregation method)**	**Soft-linking**	**Hard-linking**	**This work**
Dynamics over consecutive hours	Only within the temporal window (temporal slice)	No	Yes	Yes	Implicitly with EnergyPLAN
Potential feedback to the IAM	Yes	Yes	No	Yes	Yes
Flexibility to include variability management options	High (can be modelled in the IAM)	High (can be modelled in the IAM)	Given by the energy model	Given by the energy model	High (can be modelled in the IAM) but must be present in the energy model
Accuracy	Low	Medium	High	Very high	Medium
Complexity	Low	Medium (easy to understand but mathematically complex)	Medium (requires a deep knowledge of both models to consistenly link them)	High (as for soft-linking but also requires to hard-code the link)	High (requires a deep knowledge of both models + advanced statistical knowledge)
Reliability of the power system	Low	Medium	High (if power flow analysis is included)	Very high (if power flow analysis is included)	High (issues are hourly checked in the energy model)

Usability and presence in IAMs	High	High	Low	Low	High
	High (in declining trend)	High	Low (recent approach)	Low (recent approach)	Not tested yet
Computational cost in the IAM	Fast	Relatively fast	Slow	Slow	Fast
Potential uncertainty analysis in the coefficients	No	No	No	No	Yes

The limitations identified during the process can be addressed in further work, which could be focused on: i) implementing parallel processing algorithms to achieve a wider scope for action in the clusterization step; ii) applying other algorithms in the step of feature selection to compare them in the selection of the inputs for the regressions (e.g., Lasso, Ridge, StepWise – both, forward, backward); iii) representing intermediate relationships of the energy chains, e.g., calculate hydrogen as the output of the regression model and then use it to estimate the next variable, in this case, the production of synthetic gas, liquid fuel and hydrogen in Industry; iv) test the approach for other regional profiles; or v) generate the input values from probability distributions and then perform an uncertainty analysis to the parameters of the MLR models. In a second stage, the application of these MLR models would be into an IAM and report a benchmarking exercise comparing it with other approaches such as the soft/hard-linking between the hourly-resolution model and the IAM.

5. CONCLUSIONS

The necessity for reaching 100% renewable and neutral decarbonized scenarios has been claimed by our society and studied in the literature. The introduction section shows some advances to realistically represent the expansion of RES exploitation and technologies to manage the imbalance between the demand and supply sides in Integrated Assessment Models (IAMs). Despite several methods that have been proposed, these models require a fast response in calculating the equations to deliver a manageable product for testing (e.g., calibration) and develop the model, as well as enhance the assessment in stakeholder engagement exercises. This has led to a new line of research, a conceptualization to link hourly-resolution energy models into IAMs through statistical annual indicators, avoiding an expensive computational load. The approach is based on combinatorial analysis and multiple linear regression (MLR) models, and EnergyPLAN for the European region is applied as a case study.

The approach has delivered plausible coefficients in the regression analysis for a wide range of values in the clusters considered to represent the technological changes of the system. The capacity factor of the onshore wind and photovoltaic solar power plants, as well as both variations in the demand for electricity and natural gas, are correctly captured.

Further work has been identified for this exciting research work. Parallel processing and improvements in the data management, as well as the usage of powerful servers, can reduce the time cost per simulation of EnergyPLAN. Additional algorithms can be introduced in the analysis of feature selection and other types of probability distributions for the MLR models. Finally, a final version of the approach should be tested in a real IAM to compare the results with other methods and across scenarios and different regions.

ACKNOWLEDGEMENTS

Research of this article has been supported by the project LOCOMOTION, funded by the European Union's Horizon 2020 research and innovation program, under grant agreement No 821105. Iñigo Capellán-Pérez acknowledges financial support from a Juan de la Cierva-Incorporación Research Fellowship of the Ministry of Science and Innovation of Spain (no. IJC2020-046215-I). The authors gratefully thank the support of Felipe Andrés Feijoo Palacios in the statistical analysis. We also kindly thank Erum Rehman for her thorough revision of the English writing of this paper.

A preliminary version of this work was presented at the 16th SDEWES Conference Dubrovnik on Monday, October 11th, in room D (Energy system analysis 1).

DECLARATION OF INTERESTS

The authors declare that they have no known competing financial interests or personal relationships that could have appeared to influence the work reported in this paper.

AUTHOR CONTRIBUTIONS

Gonzalo Parrado-Hernando: Conceptualization, Methodology, Software, Formal analysis, Writing-Original Draft, Visualization **Luka Herc:** Methodology, Data curation, Software, Formal analysis, Writing-Original Draft, Visualization **Antun Pfeifer:** Conceptualization, Methodology, Writing-Original Draft, Supervision **Iñigo Capellán-Perez:** Conceptualization, Methodology, Writing-Original Draft, Supervision **Ilija Batas Bjelić:** Conceptualization, Methodology, Writing-Original Draft, Supervision **Neven Duić:** Conceptualization, Supervision **Fernando Frechoso-Escudero:** Writing-Review&Editing, Supervision **Luis Javier Miguel González:** Conceptualization, Supervision **Vladimir Z. Gjorgievski:** Conceptualization, Writing-Review&Editing.

REFERENCES

[1] European Commission, "A Clean Planet for all. A European long-term strategic vision for a prosperous, modern, competitive and climate neutral economy," *Com(2018) 773*, p. 114, 2018, [Online]. Available: https://eur-lex.europa.eu/legal-content/EN/TXT/PDF/?uri=CELEX:52018DC0773&from=EN.

[2] P. A. Østergaard, N. Duic, Y. Noorollahi, H. Mikulcic, and S. Kalogirou, "Sustainable development using renewable energy technology," *Renew. Energy*, vol. 146, pp. 2430–2437, 2020, doi: 10.1016/j.renene.2019.08.094.

[3] P. A. Østergaard, N. Duic, Y. Noorollahi, and S. A. Kalogirou, “Recent advances in renewable energy technology for the energy transition,” *Renew. Energy*, vol. 179, pp. 877–884, 2021, doi: 10.1016/j.renene.2021.07.111.

[4] E. Hillberg Antony Zegers, B. Herndler, S. Wong, J. Pompee, J.-Y. Bourmaud, and S. Lehnhoff, “Power Transmission & Distribution Systems Flexibility needs in the future power system Discussion paper,” no. February, 2019.

[5] Z. A. Obaid, L. M. Cipcigan, L. Abrahim, and M. T. Muhssin, “Frequency control of future power systems: reviewing and evaluating challenges and new control methods,” *J. Mod. Power Syst. Clean Energy*, vol. 7, no. 1, pp. 9–25, 2019, doi: 10.1007/s40565-018-0441-1.

[6] S. Djørup, J. Z. Thellufsen, and P. Sorknæs, “The electricity market in a renewable energy system,” *Energy*, vol. 162, pp. 148–157, 2018, doi: 10.1016/j.energy.2018.07.100.

[7] C. Unterberger *et al.*, “Spring frost risk for regional apple production under a warmer climate,” *PLoS One*, vol. 13, no. 7, p. e0200201, May 2018, doi: 10.1371/journal.pone.0200201.

[8] J. López Prol, K. W. Steininger, and D. Zilberman, “The cannibalization effect of wind and solar in the California wholesale electricity market,” *Energy Econ.*, vol. 85, p. 104552, 2020, doi: 10.1016/j.eneco.2019.104552.

[9] V. Bianco, O. M. Driha, and M. Sevilla-Jiménez, “Effects of renewables deployment in the Spanish electricity generation sector,” *Util. Policy*, vol. 56, pp. 72–81, Jul. 2019, doi: 10.1016/j.jup.2018.11.001.

[10] K. K. Iychettira, “Lessons for renewable integration in developing countries: The importance of cost recovery and distributional justice,” *Energy Res. Soc. Sci.*, vol. 77, no. May 2020, p. 102069, 2021, doi: 10.1016/j.erss.2021.102069.

[11] B. Matek and K. Gawell, “The benefits of baseload renewables: A misunderstood energy technology,” *Electr. J.*, vol. 28, no. 2, pp. 101–112, 2015, doi: 10.1016/j.tej.2015.02.001.

[12] W. Nordhaus, *Integrated economic and climate modeling*, vol. 1. Elsevier, 2013.

[13] U. U. R. Zia, M. Zulfiqar, U. Azram, M. Haris, M. A. Khan, and M. O. Zahoor, “Use of Macro/Micro Models and Business Intelligence tools for Energy Assessment and Scenario based Modeling,” *2019 4th Int. Conf. Emerg. Trends Eng. Sci. Technol. ICEEST 2019*, 2019, doi: 10.1109/ICEEST48626.2019.8981691.

[14] I. Capellán-Pérez *et al.*, “MEDEAS: A new modeling framework integrating global biophysical and socioeconomic constraints,” *Energy Environ. Sci.*, vol. 13, no. 3, pp. 986–1017, 2020, doi: 10.1039/c9ee02627d.

[15] M. Sugiyama *et al.*, “Japan’s long-term climate mitigation policy: Multi-model assessment and sectoral challenges,” *Energy*, vol. 167, no. 2019, pp. 1120–1131, 2019, doi: 10.1016/j.energy.2018.10.091.

[16] F. Lamperti, G. Dosi, M. Napoletano, A. Roventini, and A. Sapio, “Climate

change and green transitions in an agent-based integrated assessment model," *Technol. Forecast. Soc. Change*, vol. 153, no. November 2019, p. 119806, 2020, doi: 10.1016/j.techfore.2019.119806.

[17] D. Huppmann *et al.*, "The MESSAGEix Integrated Assessment Model and the ix modeling platform (ixmp): An open framework for integrated and cross-cutting analysis of energy, climate, the environment, and sustainable development," *Environ. Model. Softw.*, vol. 112, no. March 2018, pp. 143–156, 2019, doi: 10.1016/j.envsoft.2018.11.012.

[18] J. Weyant, "Some contributions of integrated assessment models of global climate change," *Rev. Environ. Econ. Policy*, vol. 11, no. 1, pp. 115–137, 2017, doi: 10.1093/reep/rew018.

[19] Intergovernmental Panel on Climate Change, *Climate Change 2022 - Mitigation of Climate Change - Summary for Policymakers (SPM)*, no. 1. 2022.

[20] S. Robertson, "Transparency, trust, and integrated assessment models: An ethical consideration for the Intergovernmental Panel on Climate Change," *Wiley Interdiscip. Rev. Clim. Chang.*, vol. 12, no. 1, pp. 1–8, 2021, doi: 10.1002/wcc.679.

[21] J. Skea, P. Shukla, A. Al Khourdajie, and D. McCollum, "Intergovernmental Panel on Climate Change: Transparency and integrated assessment modeling," *Wiley Interdiscip. Rev. Clim. Chang.*, vol. 12, no. 5, pp. 1–11, 2021, doi: 10.1002/wcc.727.

[22] S. Pfenninger, "Dealing with multiple decades of hourly wind and PV time series in energy models: A comparison of methods to reduce time resolution and the planning implications of inter-annual variability," *Appl. Energy*, vol. 197, pp. 1–13, 2017, doi: 10.1016/j.apenergy.2017.03.051.

[23] S. Ludig, M. Haller, E. Schmid, and N. Bauer, "Fluctuating renewables in a long-term climate change mitigation strategy," *Energy*, vol. 36, no. 11, pp. 6674–6685, 2011, doi: 10.1016/j.energy.2011.08.021.

[24] F. Ueckerdt *et al.*, "Representing power sector variability and the integration of variable renewables in long-term energy-economy models using residual load duration curves," *Energy*, vol. 90, pp. 1799–1814, Dec. 2015, doi: 10.1016/j.energy.2015.07.006.

[25] R. C. Pietzcker *et al.*, "System integration of wind and solar power in integrated assessment models: A cross-model evaluation of new approaches," *Energy Econ.*, vol. 64, no. 2017, pp. 583–599, 2017, doi: 10.1016/j.eneco.2016.11.018.

[26] J. E. T. Bistline, "The importance of temporal resolution in modeling deep decarbonization of the electric power sector," *Environ. Res. Lett.*, vol. 16, no. 8, 2021, doi: 10.1088/1748-9326/ac10df.

[27] E. J. Hoevenaars and C. A. Crawford, "Implications of temporal resolution for modeling renewables-based power systems," *Renew. Energy*, vol. 41, pp. 285–293, 2012, doi: 10.1016/j.renene.2011.11.013.

[28] B. Shirizadeh and P. Quirion, "Do multi-sector energy system optimization

models need hourly temporal resolution? A case study with an investment and dispatch model applied to France," *Appl. Energy*, vol. 305, no. April 2021, p. 117951, 2022, doi: 10.1016/j.apenergy.2021.117951.

[29] M. Howells *et al.*, "OSeMOSYS: The Open Source Energy Modeling System. An introduction to its ethos, structure and development.," *Energy Policy*, vol. 39, no. 10, pp. 5850–5870, 2011, doi: 10.1016/j.enpol.2011.06.033.

[30] M. Welsch *et al.*, "Incorporating flexibility requirements into long-term energy system models - A case study on high levels of renewable electricity penetration in Ireland," *Appl. Energy*, vol. 135, pp. 600–615, 2014, doi: 10.1016/j.apenergy.2014.08.072.

[31] H. K. Ringkjøb, P. M. Haugan, and I. M. Solbrekke, "A review of modelling tools for energy and electricity systems with large shares of variable renewables," *Renew. Sustain. Energy Rev.*, vol. 96, no. August, pp. 440–459, 2018, doi: 10.1016/j.rser.2018.08.002.

[32] Y. Scholz, H. C. Gils, and R. C. Pietzcker, "Application of a high-detail energy system model to derive power sector characteristics at high wind and solar shares," *Energy Econ.*, vol. 64, pp. 568–582, 2017, doi: 10.1016/j.eneco.2016.06.021.

[33] M. Brinkerink, "PLEXOS-World - MESSAGEix-GLOBIOM Soft-Link." Harvard Dataverse, doi: doi:10.7910/DVN/O6ICJP.

[34] R. Loulou and M. Labriet, "ETSAP-TIAM: The TIMES integrated assessment model Part I: Model structure," *Comput. Manag. Sci.*, 2008, doi: 10.1007/s10287-007-0046-z.

[35] R. Loulou, "ETSAP-TIAM: The TIMES integrated assessment model. Part II: Mathematical formulation," *Comput. Manag. Sci.*, vol. 5, no. 1–2, pp. 41–66, 2008, doi: 10.1007/s10287-007-0045-0.

[36] A. Pina, C. A. Silva, and P. Ferrão, "High-resolution modeling framework for planning electricity systems with high penetration of renewables," *Appl. Energy*, vol. 112, pp. 215–223, Dec. 2013, doi: 10.1016/j.apenergy.2013.05.074.

[37] J. P. Deane, A. Chiodi, M. Gargiulo, and B. P. Ó Gallachóir, "Soft-linking of a power systems model to an energy systems model," *Energy*, vol. 42, no. 1, pp. 303–312, Dec. 2012, doi: 10.1016/j.energy.2012.03.052.

[38] M. Brinkerink and P. Deane, "PLEXOS-World 2015." Harvard Dataverse, 2020, doi: doi/10.7910/DVN/CBYXBY.

[39] P. Harrington, *Machine Learning in Action*, vol. 37, no. 3. 2012.

[40] H. Lund and J. Z. Thellufsen, "EnergyPLAN - Advanced Energy Systems Analysis Computer Model (Document Version 15.1)," no. September, pp. 1–189, 2020, Accessed: Dec. 13, 2021. [Online]. Available: https://www.energyplan.eu/.

[41] H. Lund, J. Z. Thellufsen, P. A. Østergaard, P. Sorknæs, I. R. Skov, and B. V. Mathiesen, "EnergyPLAN – Advanced analysis of smart energy systems," *Smart Energy*, vol. 1, p. 100007, 2021, doi: 10.1016/j.segy.2021.100007.

[42] P. A. Østergaard, “Reviewing EnergyPLAN simulations and performance indicator applications in EnergyPLAN simulations,” *Appl. Energy*, vol. 154, pp. 921–933, 2015, doi: 10.1016/j.apenergy.2015.05.086.

[43] D. Connolly, H. Lund, B. V. Mathiesen, and M. Leahy, “A review of computer tools for analysing the integration of renewable energy into various energy systems,” *Appl. Energy*, vol. 87, no. 4, pp. 1059–1082, 2010, doi: 10.1016/j.apenergy.2009.09.026.

[44] H. Lund and J. Z. Thellufsen, “EnergyPLAN | Advanced energy systems analysis computer model,” 2020. https://www.energyplan.eu/ (accessed May 11, 2021).

[45] G. Parrado-Hernando *et al.*, “WILIAM Task 7.4,” Oct. 2021, doi: 10.5281/zenodo.5602814.

[46] A. Pfeifer, L. Herc, I. Batas Bjelić, and N. Duić, “Flexibility index and decreasing the costs in energy systems with high share of renewable energy,” *Energy Convers. Manag.*, vol. 240, 2021, doi: 10.1016/j.enconman.2021.114258.

[47] “Home.” https://www.entsoe.eu/ (accessed Nov. 30, 2021).

[48] M. Pavičević, T. Novosel, T. Pukšec, and N. Duić, “Hourly optimization and sizing of district heating systems considering building refurbishment – Case study for the city of Zagreb,” *Energy*, vol. 137, pp. 1264–1276, 2017, doi: 10.1016/j.energy.2017.06.105.

[49] “Renewables.ninja.” https://www.renewables.ninja/ (accessed Nov. 30, 2021).

[50] IRENA, “IRENA database,” International Renewable Energy Agency, http://resourceirena.irena.org, 2020. [Online]. Available: http://resourceirena.irena.org.

[51] F. Dalla-Longa *et al.*, *Wind potentials for EU and neighbouring countries - Input datasets for the JRC-EU-TIMES Model*. 2018.

[52] A. Jäger-Waldau, “The Untapped Area Potential for Photovoltaic Power in the European Union,” *Clean Technol.*, vol. 2, no. 4, pp. 440–446, 2020, doi: 10.3390/cleantechnol2040027.

[53] A. L. Sockloff, “The Analysis of Nonlinearity Via Linear Regression with Polynomial and Product Variables: An Examination,” *Rev. Educ. Res.*, vol. 46, no. 2, pp. 267–291, 1976, doi: 10.3102/00346543046002267.

[54] S. Collins *et al.*, “Integrating short term variations of the power system into integrated energy system models: A methodological review,” *Renew. Sustain. Energy Rev.*, vol. 76, pp. 839–856, Dec. 2017, doi: 10.1016/j.rser.2017.03.090.

[55] A. V. Pastor, D. C. S. Vieira, F. H. Soudijn, and O. Y. Edelenbosch, “How uncertainties are tackled in multi-disciplinary science? A review of integrated assessments under global change,” *Catena*, vol. 186, no. September 2019, p. 104305, 2020, doi: 10.1016/j.catena.2019.104305.

[56] F. Ueckerdt, R. Pietzcker, Y. Scholz, D. Stetter, A. Giannousakis, and G. Luderer, “Decarbonizing global power supply under region-specific

consideration of challenges and options of integrating variable renewables in the REMIND model," *Energy Econ.*, vol. 64, pp. 665–684, 2017, doi: 10.1016/j.eneco.2016.05.012.

[57] B. J. M. de Vries, D. P. van Vuuren, and M. M. Hoogwijk, "Renewable energy sources: Their global potential for the first-half of the 21st century at a global level: An integrated approach," *Energy Policy*, vol. 35, no. 4, pp. 2590–2610, Apr. 2007, doi: 10.1016/j.enpol.2006.09.002.

[58] D. P. van Vuuren, *Energy systems and climate policy - Long-term scenarios for an uncertain future*. 2007.

[59] S. Fujimori, T. Hasegawa, and T. Masui, "AIM/CGE V2.0: Basic Feature of the Model," in *Post-2020 Climate Action. Global and Asian Perspectives*, S. Fujimori, M. Kainuma, and T. Masui, Eds. Singapore: Springer, 2017, pp. 305–328.

[60] H. Dai, S. Fujimori, D. Silva Herran, H. Shiraki, T. Masui, and Y. Matsuoka, "The impacts on climate mitigation costs of considering curtailment and storage of variable renewable energy in a general equilibrium model," *Energy Econ.*, vol. 64, no. 2017, pp. 627–637, 2017, doi: 10.1016/j.eneco.2016.03.002.

[61] M. Binsted *et al.*, "GCAM-USA v5.3_water_dispatch: Integrated modeling of subnational U.S. energy, water, and land systems within a global framework," *Geosci. Model Dev. Discuss.*, no. July, pp. 1–39, 2021, doi: 10.5194/gmd-2021-197.

[62] Z. Khan *et al.*, "Impacts of long-term temperature change and variability on electricity investments," *Nat. Commun.*, vol. 12, no. 1, pp. 1–12, 2021, doi: 10.1038/s41467-021-21785-1.

[63] I. Capellán-Pérez, C. de Castro, and L. J. Miguel González, "Dynamic Energy Return on Energy Investment (EROI) and material requirements in scenarios of global transition to renewable energies," *Energy Strateg. Rev.*, vol. 26, no. September, p. 100399, 2019, doi: 10.1016/j.esr.2019.100399.

[64] L. Baumstark *et al.*, "REMIND2.1: Transformation and innovation dynamics of the energy-economic system within climate and sustainability limits," *Geosci. Model Dev. Discuss.*, pp. 1–50, 2021, doi: 10.5194/gmd-2021-85.

[65] J. Després, K. Keramidas, A. Schmitz, A. Kitous, and B. Schade, *POLES-JRC model documentation*. 2018.

[66] I. Energy, "MESSAGEix-GLOBIOM," 2021.

[67] P. Sullivan, V. Krey, and K. Riahi, "Impacts of considering electric sector variability and reliability in the MESSAGE model," *Energy Strateg. Rev.*, vol. 1, no. 3, pp. 157–163, 2013, doi: 10.1016/j.esr.2013.01.001.

[68] R. C. Pietzcker, D. Stetter, S. Manger, and G. Luderer, "Using the sun to decarbonize the power sector: The economic potential of photovoltaics and concentrating solar power," *Appl. Energy*, vol. 135, pp. 704–720, 2014, doi: 10.1016/j.apenergy.2014.08.011.

[69] D. Arent *et al.*, “Improved Offshore Wind Resource Assessment in Global Climate Stabilization Scenarios,” *Natl. Renew. Energy Lab.*, no. October, p. 29, 2012, [Online]. Available: https://www.nrel.gov/docs/fy13osti/55049.pdf.

[70] S. Carrara and G. Marangoni, “Including System Integration of Variable Renewable Energies in a Constant Elasticity of Substitution Framework: The Case of the WITCH Model,” *SSRN Electron. J.*, 2016, doi: 10.2139/ssrn.2718136.

[71] T. L. Vu and K. Turitsyn, “A Framework for Robust Assessment of Power Grid Stability and Resiliency,” *IEEE Trans. Automat. Contr.*, vol. 62, no. 3, pp. 1165–1177, 2017, doi: 10.1109/TAC.2016.2579743.

APPENDICES

APPENDIX A

Table A. 1. Presence of VRES, methods used to explicitly represent the potential production of VRES, and methods used to explicitly represent the power system operation with the presence of VRES in IAMs. Abbreviations: Abbreviations: CF: Capacity Factor. GIS: Geographical Information System mapping. CF: Capacity Factor. *GIS:* Geographical Information System mapping. *MOS:* Merit Order Strategy. *CES:* Constant Elasticity Substitution. *MNL:* Multinomial Logit function. Own elaboration.

Time resolution / Model	IMAGE (IAM)	AIM/CGE (IAM)	GCAM (IAM)	MEDEAS (IAM)	REMIND-MAgPIE (IAM)	POLES (Energy model)	MESSAGEix-GLOBIOM (IAM)	WITCH-GLOBIOM (IAM)
VRES technologies	Wind onshore and solar-PV	Wind onshore and solar-PV	Wind onshore, wind offshore and solar-PV	Solar-PV, wind onshore, and wind offshore	Solar-PV, wind (not specified), run-of-river hydropower	Wind (not specified), solar-PV, run-of-river hydropower, marine, solar CSP (with or without heat storage)	Wind onshore, wind offshore, solar-PV	Wind onshore, wind offshore, solar-PV
Sub-annual / hourly			Sub-annual load profiles			Hourly production profiles derived from techno-physical potentials and installed capacities	Linear downscaling for soft-linking in hourly resolution	

Yearly	Exogenous supply curve from GIS study	Installed capacity based on official reports	Exogenous resource supply curve and installed capacity	Curtailment and installed capacity (up to maximum potential)	Region-specific potentials with different grades of CF, and installed capacity		Exogenous supply curve and CF based on technological penetration	Supply curves (CF qualities) and installed capacity
Technical side	Dispatch RLDC with 156-time slices.	Region-wide pooling contained ex ante in the RLDC.		Dispatch based on exogenous priorities & endogenous EROI	Dispatch according to RLDC with 4 load bands	Investment RLDC only has a country-level pool	Partial equilibrium and load factors (capacity reserve and flexibility requirements) Power grid reliability (soft-linking) at an hourly level	Decisions based on priorities constrained by CF

Economical side	Decision-based MOS based on operational costs.	MNL function based on generation prices.	Competition based on the linearly optimal least-cost approach in 25 sub-annual time segments (monthly day/night + super peak)		Optimization of generation cost by technology	Hourly decision based on priorities in representative days (12 days for EU-27; 2 for the rest). Residual technologies compete in terms of variable generation costs.		Constant elasticity of substitution functions of costs.

Table A. 2. Flexibility options present in IAMs. DSM: Demand-Side Management. V2G: Vehicle-to-Grid. P2H: Power-to-Heat. Own elaboration.

Models / Flexibility options	IMAGE	AIM/CGE	GCAM	MEDEAS	REMIND-MAgPIE	POLES	MESSAGEix-GLOBIOM	WITCH-GLOBIOM
Demand-side management						X		
V2G connection						X		
Electrolyzers to produce hydrogen					X	X	X	
Grid electric batteries	X	X		X	X	X		
Storage (pumped hydropower, compressed air storage, etc)				X		X	X	X
Power-to-heat					X			
Curtailment	X	X		X	X	X		
Back-up dispatchable generation	X	X	X	X	X	X	X	X

Following these lines, the models analyzed in the literature review are briefly described.

IMAGE – Integrated Model to Assess the Global Environment

The potential supply of solar and wind onshore power are estimated from a GIS study (0.5 x 0.5 degree) to relate the installed capacity with the capacity factor [57]. There is no differentiation between wind onshore and offshore, however, only the potential of the first one has been carried out.

IMAGE works with monthly load duration curve (LDC) from exogenous regional factors. Investments and generation costs allow for competition between technologies to increase their share in the capacity park. Dispatch of electricity is based on merit order strategy. VRES have priority, then baseload is assigned based multinomial logit model, and finally, the peak is fulfilled through the same model (multinomial logit).

Three are the effects of VRES in the IMAGE model. When curtailment, the load factor is reduced, and costs are increased. Beyond 5% of VRES penetration, capacity credit decreases so back-up power is then required, generating an extra cost that is allocated to the variable renewable technology. Another effect is related to the spinning reserve. IMAGE assumes a minimum of 3.5% plus 15% of VRES installed capacity. So, total reserves are increased just in case the additional spinning reserves exceed the capacity of reserves already installed [58], if so, costs are again allocated to the intermittent technology.

More recently, the RLDC approach has been applied to this model [25]. Resolution changed from monthly LDCs to 156-time slices. Flexibility, ramping, adequacy and curtailment are addressed now under the new method. Exogenous investments for electric storage-based VRES share appeared in the article [25].

AIM/CGE – Asia-Pacific Integrated Model/Computable General Equilibrium

It is an econometric model. Availability (installed capacity) and cost of VRES are exogenously introduced from official reports. The power supply is annually solved by employing logit function and generation prices, providing the shares by technology that contributes to satisfying the annual demand. Exponents of logit functions are calibrated and exogenously introduced for future scenarios. The decreasing trend for the price of electricity generated by renewables is assumed [59] (section 13.3. Energy Supply); however, intermediate trade of inputs, labour, and capital cost are included, so power sector cost can be estimated.

Later, two studies have improved the complexity of that power system. On the one hand, storage and curtailment have been represented through exponential equations whose parameters were estimated using the least-squares method [60] for regional and hourly LDC data from another study [56]. The use of intermediate trade allows for including costs for using storage since the devices need to be provided by another sector.

GCAM – Global Change Analysis Model

The model written in GAMS (open-source version available on GitHub) represents the investment decisions by using a probabilistic logit formulation to foster or not the expansion of supply generation units in four different representative segments (peak, subpeak, intermediate, baseload). 15% of the reserve margin is considered.

Availability of resources is given by exogenous supply curves. Twenty-five sub-annual load profiles (one per day and night each month and a super-peak considering the top 10 hours in the year) [61]. A specific version of GCAM [62] disaggregates the electricity demand load by end-use sector (transportation, buildings, and industry).

MEDEAS – Modelling the Energy Development under Environmental And Socioeconomic Constraints

This system dynamics model (Vensim software with an open-source version in Python) works on a yearly basis. Exogenous potentials are introduced as maximum installed capacities of technologies. Then, CF delivers the potential electricity generated by technology. Capacity factors of VRES technologies are dynamized with damage functions according to the penetration of such variable sources into the power system (section 2.2. of Supplementary Material in [63]).

The operation of the power sector is represented by constant priorities up to fulfilling the demand (by order: VRES, nuclear, dispatchable renewables, and then dispatchable fossil power plants).

REMIND/MAgPIE – Regional Model of Investment and Development/Model of Agricultural Production and its Impact on the Environment

REMIND models the regional potential of non-biomass renewables employing a grade of capacity factors in which superior grades correspond to more full-load hours per year. It runs in 5-year steps from 2005 to 2060, then 10 years up to the end of the century. A constraint is defined to remain the coherently combined deployment of both solar-PV and -CSP in the same region [64].

The integration of VRES (solar-PV, wind, and run-of-river hydropower) in REMIND takes away a couple of effects. Integration costs and curtailment are parameterized from the REMIx (integration costs) [32] and DIMES (RLDCs – 4 bands: peak, higher mid, lower mid, and base; plus 2 additional variables for maximum peak load and curtailment – containing the impact of storage) [56]. This optimization model assumes a single electricity market balance. Optimization is carried out to show the least cost configuration of the power system.

REMIND considers several flexibility options. Storage requirement is determined by the share and the profile of renewable production, as well as the curtailment present in the year. Power-to-heat may be promoted but limited by the spatial observed data. Finally, hydrogen can be used to reduce curtailment and flexible the power system operation. The effect of additional grid capacity is also considered and connected to the VRES (wind and solar) capacity and regional spatial differences.

POLES – Prospective Outlook on Long-term Energy Systems

Generation of VRES is defined by production profiles, calculated from the potential of the technology available (derived, in turn, from the meteorological and technical potentials and land-use exclusion factors) and costs [65].

Operation by priority. Decentralized production is firstly allocated (solar-PV, solar CSP, small hydro, and stationary fuel cells) in competition with the retail electricity price. Secondly, non-dispatchable centralized power plants (wind, large solar, hydro run-of-river, marine). Thirdly, nuclear and dam hydropower plants (short flexibility rates) [65].

On the negative part of RLDC, some demanders may mitigate the variability. Exports, hydrogen production, smart mode of electric vehicles, and other storage facilities (pumping hydropower plants, stationary batteries, compressed air energy storage, and demand-side management). Finally, curtailment would remain. The remaining technologies compete based on variable costs of generation [65].

MESSAGEix/GLOBIOM – Model of Energy Supply Systems And their General Environmental Impact/Global Biosphere Management Model

MESSAGEix is the energy modeling of this IAM, open-source and based on optimization of computable general equilibrium formulation.

Quality of the regional resource potentials of VRES is exogenously introduced in terms of annual CF based on technical, sustainability, and economic criteria [66].

A stylized approach [67] sizes the operational reliability through two metrics. On the one hand, capacity reserves to match a peak load (estimated at 1.7 times the average) and a standard reserve margin of between 15-20%. The penalty on the CF of VRES is also computed according to the penetration of these technologies in the power system. On the other hand, flexibility parametrization to different technologies (negative values for VRES) is based on an hourly unit commitment model.

Storage (pumped hydropower, compressed air storage, flow batteries) and demand-side technologies to produce hydrogen (electrolyzers) add flexibility to the power system. Flexibility is modeled through negative and positive parameters. Negative ones increase the stiffness of the system operation, i.e., VRES and demand. On the other counterpart, the dispatchable power supply is flexible, so technologies under this category are positive, e.g., diesel engine, combined cycle gas turbine, electrolyzers, and so on.

A recent experience of soft-linking with the PLEXOS-world model achieved hourly resolution on the operation side and expansion of the transmission grid for the IAM [33].

WITCH/GLOBIOM – World Induced Technical Change Hybrid Model/ Global Biosphere Management Model

The supply curve for solar-PV is considered from the same analysis for the REMIND model [68], delivering the maximum amount of capacity which can be installed by region, in terms of capacity factor or full load hours in the year. Different classes are sorted by quality and distances from the load centers. Similarly, the supply curve of wind onshore and offshore is modeled in the same way but data comes from the NREL laboratory [69].

Elasticities of substitution based on costs are the core of WITCH to reflect internal changes in the electricity sector.

Two constraints are introduced to manage VRES variability. Firstly, flexibility constraints ensure that suppliers can handle load fluctuations. In order to reflect that, a flexibility parameter (between -1 and 1) is assumed by a supplier, where negative values add inflexible production and positive values include flexible production. Annually, production must be positively balanced. Secondly, the capacity constraint guarantees the match of the peak load demand (so-called firm capacity) in between 1.5-2 times (regional differences) the average load demand (annual demand divided by 8760 hours, so the mean hourly capacity, assuming the equivalence MWh – MW in the hour) [70].

Penalty on the CF of VRES technologies is considered to render the effect of increasing rates of VRES capacity in the system, as well as storage requirements.

APPENDIX B

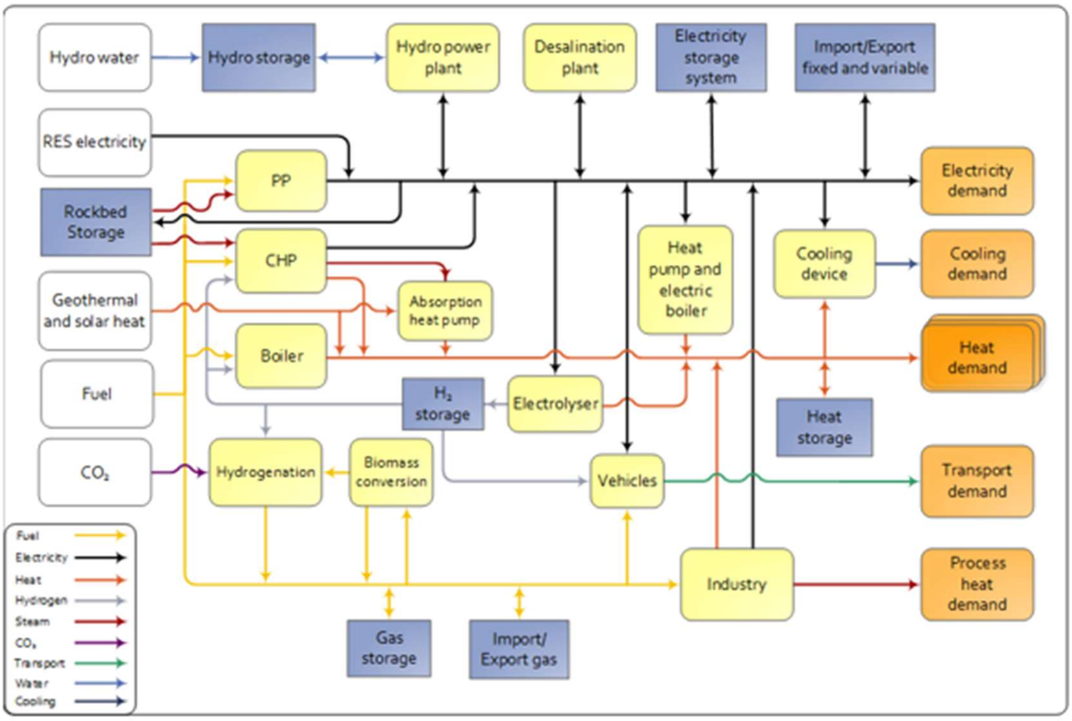

Figure B. 1. General diagram of the EnergyPLAN, version 15.1 (15 September 2020) [44].

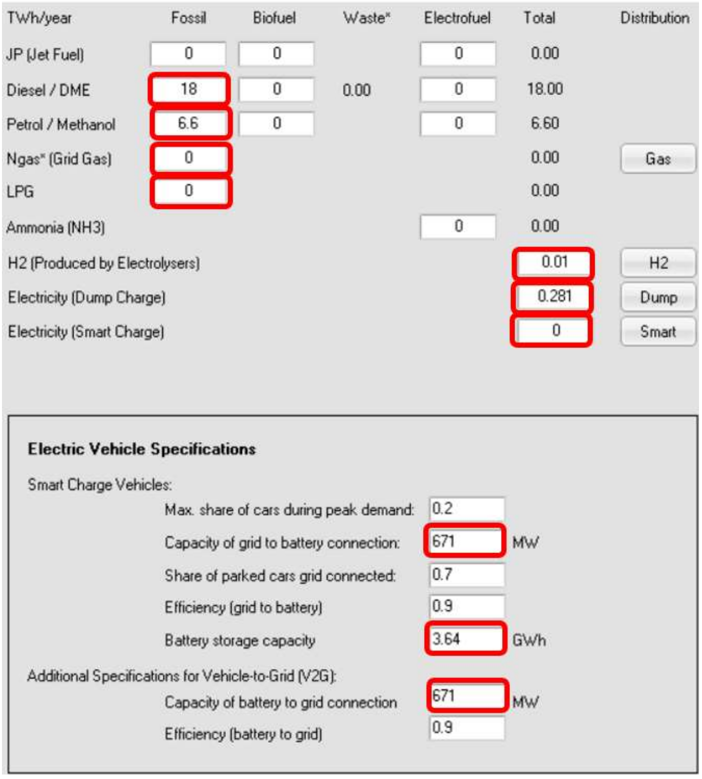

Figure B. 2. Inputs in EnergyPLAN relating to the transport module.

1234 Table B. 1. List of flexibility options, definitions, and own estimations for the approach proposed

Acronyms	Definition	Own estimations
Baseload	Flexible operation of thermal and nuclear power plants.	The baseline minimum operating capacity of power plants is estimated to be 20 % of the nominal capacity of existing power plants. This corresponds to 67817 MW in PP and 24397 MW in CHP. Therefore, in the cases representing the development of an energy system, the minimum operating capacity is reduced to 50 % of current capacity as well as to 0 % of current capacity representing fully flexible thermal power plants.
ElecTransport	Transport electrification and V2G technology.	The baseline configuration of the fuel use in the transport sector is taken from historical data representing the year 2017. The cases representing future development consider the decrease of fossil fuel use and shift to electricity-based transport.
Storage	Energy storage systems: pumped hydropower (PHS), stationary batteries, and rock-bed storage.	The capacity for energy storage in batteries, rock-bed storage and pumped hydro storage accounts for 20 hours of average electricity demand. The maximum storage capacities account for 500 GWh in battery storage, 1600 GWh in rock bed storage, and up to 5000 GWh in PHS storage. The biggest role is given to the PHS due to the availability of favorable geographical features as well as rock beds for similar reasons, especially in mountainous regions. The smaller capacity is given to stationary battery storage due to concerns about mineral supply and because the highest emphasis is given to the batteries in electric vehicles. This notion ties again with the merit order of technologies in EnergyPLAN where the V2G is utilized more frequently than stationary storage. Therefore, the resources are put to better purpose if implemented into vehicles.
P2H	Power-to-heat. Devices to transform electricity to heat.	Power to heat is considered in the realm of district heating systems. The capacity is considered in the range from 10 000 MW to 100 000 MW which by capacity corresponds up to 25 % of district heating peak load. Also, additional reasoning for the use of such limitation is the used version of EnergyPLAN
FossilIndustry	Decarbonization of industry with hydrogen and electricity.	The industry sector is simplified for the simulations. The fossil fuel-based energy demand is represented solely by natural gas. The sector is decarbonized with the implementation of hydrogen and electricity which replaces natural gas. Natural gas has the reference energy demand of 2090 TWh in the industry sector and is being able to be completely replaced by electricity and hydrogen.

SynthGas	Generation of synthetic gas	Another way of decarbonizing the energy system is by the introduction of synthetic gas. The used values in the simulations are only 0 and 1000 TWh since no additional emphasis is given to the more widespread use of this technology. The use of this technology is partially interchangeable with the decarbonization of industry, but it is much more energy-intensive since it requires further processing to generate synthetic gas as opposed to the pure hydrogen.
DSM	Demand-side Management. Flexibilization of electricity demand.	Flexible demand is assumed to account for maximum of up to 50 % of basic electricity demand. Out of total flexible demand, 40 % is assumed to be within the 24 hours and 30 % both in a weekly and monthly periods.
GridStability	System stability parameter	The used values for this parameter are 0 and 0.3. The parameter describes the minimum share of energy sources able to provide ancillary services which must be in operation at any given time in the system. Legacy energy systems rely heavily on spinning reserve and rotating masses to ensure grid stability[‡] with the provision of such services. With advancements in energy electronics, this problem can be managed even without the large-scale implementation of spinning reserves. The reason for the decrease of this parameter is because spinning reserve comes from thermal power plants and hydropower plants which then must be kept in any system architecture. But it is not realistic to insist on this kind of legacy inertia when the majority of electricity generation comes from VRES. Which can provide artificial inertia as ancillary services.

[‡] We use the definition from EnergyPLAN documentation, which might be translated as the *"share of total electricity production in every hour that must come from a dispatchable power plant, i.e., units with flexible power output"*. This parameter encloses a set of assumptions in effects such as ramp constraints and reliability on voltage and frequency that are more properly studied in temporal resolutions close to milliseconds [71].

Table B. 2. Characteristics of the inputs for combinations and clusters.

Cluster	Input	Definition	Units	Point values
Wind	Wind [MW]	The capacity of wind power plants in the region.	MW	500000, 1000000, 1500000, 2000000, 2500000
	Offshore wind [MW]	The capacity of offshore wind power plants in the region.	MW	50000, 100000, 150000, 200000, 250000
Solar	PV [MW]	The capacity of solar-photovoltaic power plants in the region.	MW	1000000, 1500000, 2000000, 2500000
	CSP [MW]	The capacity of concentrated solar power plants in the region.	MW	20000, 40000, 60000, 80000
Geothermal	Geothermal [MW]	Capacity of geothermal power plants	MW	1000,50000, 100000
Baseload	PPminimum [MW]	Minimum operating capacity in Power Plants (PP1/PP2 in EnergyPLAN)	MW	0, 33908.5, 67817
	CHPminimum [MW]	Minimum operating capacity in cogeneration power Plants (CHP in EnergyPLAN)	MW	0, 12198.5, 24397
	Nuclear part load [-]	Flexibility share of nuclear power plants (totally rigid = 1)	-	0, 0.5, 1
	Electrification and V2G share	Electrification of the transport sector as a share	-	0.05, 0.5, 1
	Jet fuel	Jet fuel consumption in transport sector	TWh/year	71.72, 35.88, 0
	Bio jet fuel	Jet biofuel consumption in transport sector	TWh/year	0.039, 35.88, 71.72
	Diesel	Diesel consumption in transport sector	TWh/year	2586.15, 968.59, 0
	Biodiesel	Biodiesel consumption in transport sector	TWh/year	26.45, 387.44, 0
ElecTranport	Petrol	Petrol consumption in transport sector	TWh/year	933.62, 309.95, 0
	Biopetrol	Biopetrol consumption in transport sector	TWh/year	6.76, 77.49, 0
	Natural gas	Gris gas (natural gas) consumption in transport sector	TWh/year	36.48, 193.72, 0

	LPG	Liquified Petrol Gas consumption in transport sector	TWh/year	70.74, 0, 0
	Electricity smart charge	Electricity demand for electric vehicles in smart charge mode	TWh/year	64.25, 581.15, 1162.3
	Storage	Storage in electric vehicles	GWh	1271.48, 11501.25 23002.5
	Charging/discharging capacity	The capacity of electric storage in the power grid	MW	186484.2, 1686850, 3373700
P2H	P2H [MW]	Power-to-heat capacity (heat pumps+electric boilers)	MW	10000, 50000, 100000
	P2H storage [GWh]	Storage of heat for power-to-heat facilities	GWh	400, 2000, 4000
Storage	Battery power capacity [MW]	The capacity of batteries in the power grid	MW	0, 50000, 100000
	Battery storage capacity [GWh]	Storage of batteries in the power grid	GWh	0, 250, 500
	PHS [MW]	The capacity of pumping mode in hydropower plants	MW	0, 50000, 100000
	PHS [GWh]	Storage in hydropower plants to the pumping mode	GWh	0, 800, 1600
	High-temperature storage [MW]	The capacity of Rockbed storage dedicated to high-temperature processes	MW	50000, 75000, 100000
	High-temperature storage [GWh]	Storage of Rockbed facilities dedicated to high-temperature processes	GWh	2500, 3750, 5000
DSM	Flexible demand [-]	Percentage of electricity demand that is flexible	%	0, 25, 50
	Day energy flexible [TWh]	Flexible electricity demand in the day	TWh/year	0, 300, 600
	Week energy flexible [TWh]	Flexible electricity demand in the week	TWh/year	0, 225, 450
	Month energy flexible [TWh]	Flexible electricity demand in the month	TWh/year	0, 225, 450
	Day power flexible [MW]	Flexible capacity in the demand side of the power system in the day	MW	0, 46100, 92200
	Week power flexible [MW]	Flexible capacity on the demand side of the power system during the week	MW	0, 34575, 69150

	Month power flexible [MW]	Flexible capacity on the demand side of the power system during the month	MW	0, 34575, 69150
FosilIndustry	Industry decarbonization [-]	Percentage of electricity-based industry processes	%	0, 0.5, 1
	Natural gas in the industry [TWh]	Natural gas in the Industry	TWh/year	2090, 1045, 0
	H2 in the industry [TWh]	Hydrogen in the Industry	TWh/year	0, 522.5, 1045
	Electricity in the industry [TWh]	Electricity in the Industry	TWh/year	0, 522.5, 1045
SynthGas	Synthetic gas [TWh]	Synthetic gas production	TWh/year	0, 1000
GridStability	Grid Stability [Dmnl]	Grid stability parameter	Dmnl	0, 0.3

Table B. 3. Characteristics of the constant inputs.

CONSTANT VALUES			
Name	Explanation	Unit	Value
River hydro	The capacity of Run-of-River hydropower plants.	MW	80000
Nuclear	The capacity of Nuclear power plants.	MW	169541.3
PP1	The capacity of back-up (traditional fossil fuels) power plants in PP1 group	MW	121985.9
PP2	The capacity of back-up (traditional fossil fuels) power plants in PP2 group		60442.3
CHP group 3	The capacity of Combined Heat and Power plants in group 3	MW	97588.72
CHP group	The capacity of Combined Heat and Power plants in group 2	MW	0
District heating in gr3	Demand of district heating in group 3.	TWh	1100

District heating in gr2	Demand of district heating in group 2	TWh	0
Natural gas in HH	Demand of natural gas in households.	TWh	0
Oil in HH	Demand of oil in households.	TWh	0
Coal in HH	Demand of coal in households.	TWh	0
Biomass in HH	Demand of biomass in households.	TWh	700
Heat pumps in HH	Demand supplied by heat pumps in households.	TWh	620
Electric boilers in HH	Demand for electricity in electric boilers in households.	TWh	150
Solar heating in HH	Supply of solar heat to the households	TWh	240
Fuels in power plants and boilers	Fuel distribution. Biomass and natural gas may be replaced by synthetic gas in case hydrogen is considered a flexibility option.		50:50
Dammed hydro	The capacity of dammed hydro power plants	MW	95621.54
Water supply	Dammed hydro power plants water supply	TWh	200.5
Electricity dump	Electricity demand for electric vehicles in dump charge mode	TWh	0
Oil industry	Oil in industry	TWh	0
Coal industry	Coal in industry	TWh	0
Regulation strategy	EnergyPLAN demand regulation strategy		892345160

APPENDIX C

Table C. 1. Independent and dependent coefficients for the MLR models.

Output / Input	Indep	Wind	Solar	DSM	ElecTransport	FossilIndustry	Geothermal	GridStability	Storage	P2H	Baseload	SynthGas	Wind_Solar	Wind_Geothermal
VarCFwindOn	-4.51759883002705	3.68072059240587		-7.15294757299932	-1.19233614245133	1.72641782605151	15.1782664933308	2.67162404522911	-12.2795932963979	-9.53026943907884		-37.5879723598354	14.3263042582598	
VarCFwindOff	-11.9048700426978				-1.98697991428340	2.95859202929348		15.7093057696786	-30.1516985814758			-69.4315309581178	25.3452476914258	
VarCFsolarPV	-7.47204307678028		3.62242958603858	-14.5923845023130	-1.41541807499874	2.09193108991946	21.3633894960933	5.54780369186252	-12.3675128522223			-45.2982139262519	26.3006488717257	
VarCFchp	-8.58569276028090	11.9731239286154	8.82640635730433		-0.184423962089583	1.14359042663306	24.0984749273926	0.492739809072430	-0.493194766652292		-58.6177366418888	-19.0598466365920	1.99507948641974	
VarCFnuclear	0.0873451526187755	1.42289714011823			-0.196507457420719	0.478241737569628	10.8533559298036	-4.17520881482007	-2.16235803321994		8.32538432895066	-7.43919016960886		
VarCFpp	1.27759383238363	-0.497092645111093			-0.177344540245201	0.389418853753712	17.2130437735043	-4.87984894855034	1.86900450173288		-24.3219607666055	-8.52930367233265		
VarCFhp	-1.95761901260798		1.34843248874067	-2.29098430085947		-0.529781726371574	-6.20612538992764	-0.809788301873015	-0.924903541847654	98.0951729236564	9.54354063650877	10.2660651098250	2.52609930725042	
VarNatGas	0.485073030576524			-0.854956239965714	-0.0514200189140126	-0.420305694205656		-0.718474095055575	0.225892661639468		-4.72321348132826	3.65232040917356	1.73481274693728	10.3859255459323
VarElecDemand	-1.73906181938716	1.64267920484489	1.63096484952781	15.7049018816037		0.348333333333371			-0.0548291262786735	-0.128405244450522	-0.121967186221387	-0.0571779004234652	-0.0628833014541462	

APPENDIX D

This appendix shows the results from the iterative process selecting the inputs for each the regression model.

Table D. 1. Inputs selected over iterations to build the regression model for the output 'VarCFwindOff'. Combined inputs (input 1 * input 2) are represented by '_'. A correlation coefficient of 0.05 was the criteria to stop the loop.

Regression input	Correlation coefficient	R-squared adjusted
GridStability	0.29	0.09
FossilIndustry	0.26	0.07
Wind_Solar	0.23	0.05
SynthGas	0.18	0.03
Storage	0.13	0.02
ElecTransport	0.09	0.01
Wind_Solar	0.11	0.01

Table D. 2. Inputs selected over iterations to build the regression model for the output ‘VarCFsolarPV’. Combined inputs (input 1 * input 2) are represented by '_'. A correlation coefficient of 0.05 was the criteria to stop the loop.

Regression input	Correlation coefficient	R-squared adjusted
Wind_Solar	0.43	0.19
FossilIndustry	0.45	0.20
GridStability	0.49	0.24
SynthGas	0.46	0.21
Solar	0.35	0.12
ElecTransport	0.38	0.14
Storage	0.22	0.05
Geothermal	0.24	0.06
DSM	0.09	0.01
Wind_Solar	0.08	0.01

Table D. 3. Inputs selected over iterations to build the regression model for the output ‘VarCFchp’. Combined inputs (input 1 * input 2) are represented by '_'. A correlation coefficient of 0.05 was the criteria to stop the loop.

Regression input	Correlation coefficient	R-squared adjusted
Baseload	0.60	0.36
Wind	0.59	0.35
FossilIndustry	0.52	0.27
SynthGas	0.53	0.29
ElecTransport	0.21	0.04
Baseload	0.24	0.06
Solar	0.18	0.03

Wind_Solar	0.24	0.06
Geothermal	0.27	0.07
Storage	0.14	0.02
GridStability	0.13	0.02
Solar	0.12	0.01
Wind_Solar	0.10	0.01
Baseload	0.06	0.00
SynthGas	0.05	0.00

Table D. 4. Inputs selected over iterations to build the regression model for the output 'VarCFnuclear'. Combined inputs (input 1 * input 2) are represented by '_'. A correlation coefficient of 0.05 was the criteria to stop the loop.

Regression input	Correlation coefficient	R-squared adjusted
GridStability	0.67	0.45
Wind	0.29	0.09
FossilIndustry	0.28	0.08
SynthGas	0.22	0.05
Geothermal	0.17	0.03
ElecTransport	0.14	0.02
Baseload	0.13	0.02
Storage	0.12	0.01

Table D. 5. Inputs selected over iterations to build the regression model for the output 'VarCFpp'. Combined inputs (input 1 * input 2) are represented by '_'. A correlation coefficient of 0.05 was the criteria to stop the loop.

Regression input	Correlation coefficient	R-squared adjusted
GridStability	0.70	0.49
Baseload	0.32	0.10
Geothermal	0.25	0.06
FossilIndustry	0.21	0.05
SynthGas	0.22	0.05
Storage	0.09	0.01
ElecTransport	0.10	0.01
Wind	0.09	0.01

Table D. 6. Inputs selected over iterations to build the regression model for the output 'VarCFhp'. Combined inputs (input 1 * input 2) are represented by '_'. A correlation coefficient of 0.05 was the criteria to stop the loop.

Regression input	Correlation coefficient	R-squared adjusted
P2H	0.83	0.68
FossilIndustry	0.27	0.07
SynthGas	0.18	0.03
Solar	0.17	0.03
GridStability	0.16	0.03
Wind_Solar	0.16	0.03

Geothermal	0.10	0.01
Baseload	0.10	0.01
Storage	0.08	0.01
Solar	0.07	0.01
DSM	0.06	0.00

Table D. 7. Inputs selected over iterations to build the regression model for the output 'VarNatGas'. Combined inputs (input 1 * input 2) are represented by '_'. A correlation coefficient of 0.05 was the criteria to stop the loop.

Regression input	Correlation coefficient	R-squared adjusted
FossilIndustry	0.64	0.41
GridStability	0.53	0.28
Baseload	0.33	0.11
SynthGas	0.36	0.13
Wind_Solar	0.33	0.11
Wind_Geothermal	0.32	0.10
ElecTransport	0.16	0.02
SynthGas	0.09	0.01
DSM	0.07	0.00
Storage	0.07	0.00

Table D. 8. Inputs selected over iterations to build the regression model for the output 'VarElecDemand'. Combined inputs (input 1 * input 2) are represented by '_'. A correlation coefficient of 0.05 was the criteria to stop the loop.

Regression input	Correlation coefficient	R-squared adjusted
DSM	0.71	0.50
FossilIndustry	0.78	0.61
Wind_Solar	0.40	0.16
Storage	0.15	0.02
DSM	0.14	0.02
P2H	0.12	0.02

Solar	0.10	0.01
Baseload	0.08	0.01
SynthGas	0.07	0.01
Wind	0.06	0.00
Wind_Solar	0.08	0.01

APPENDIX E

The tables of this section summarize t-statistic hypothesis tests for the outputs of interest. SE: square errors explained by the term. tStat: t-statistic. Finally, the p-value of the t-statistic value is written in the last column.

Table E. 1. Hypothesis test on t-statistics for the output 'VarCFwindOff'.

Regression input	SE	tStat	p-value
ElecTransport	0.25	-47.09	0
FossilIndustry	0.07	-29.23	8.03e-188
GridStability	0.07	45.06	0
Storage	0.54	29.26	3.62e-188
SynthGas	0.89	-33.77	5.46e-250
Wind_Solar	1.89	-36.69	1.09e-294

Table E. 2. Hypothesis test on t-statistics for the output 'VarCFsolarPV'.

Regression input	SE	tStat	p-value
DSM	0.62	-23.58	6.46e-123
ElecTransport	0.02	-73.91	0
FossilIndustry	0.02	114.90	0
Geothermal	0.71	30.21	1.69e-200
GridStability	0.05	113.42	0
Solar	0.07	53.43	0
Storage	0.23	-53.47	0
SynthGas	0.46	-97.83	0
Wind_Solar	0.32	82.88	0

Table E. 3. Hypothesis test on t-statistics for the output 'VarCFchp'.

Regression input	SE	tStat	p-value

Baseload	0.57	-102.63	0
ElecTransport	0.01	-13.75	5.30e-43
FossilIndustry	0.01	82.19	0
Geothermal	0.59	41.09	0
GridStability	0.04	13.33	1.58e-40
Solar	0.24	36.18	1.47e-286
Storage	0.17	-2.89	3.90e-3
SynthGas	0.31	-61.47	0
Wind_Solar	0.25	48.07	0

Table E. 4. Hypothesis test on t-statistics for the output ' VarCFnuclear'.

Regression input	SE	tStat	p-value
Baseload	0.48	17.37	1.48e-67
ElecTransport	0.01	-17.10	1.43e-65
FossilIndustry	0.01	38.22	1.20e-319
Geothermal	0.46	23.83	1.55e-125
GridStability	0.03	-122.24	0
Storage	0.14	-15.21	2.82e-52
SynthGas	0.27	-27.79	5.23e-170
Wind	0.04	35.91	2.19e-282

Table E. 5. Hypothesis test on t-statistics for the output ' VarCFpp'.

Regression input	SE	tStat	p-value
Baseload	0.49	-49.15	0
ElecTransport	0.01	-15.05	3.69e-51
FossilIndustry	0.01	30.41	4.41e-203

Geothermal	0.47	36.66	3.30e-294
GridStability	0.04	-138.44	0
Storage	0.15	12.78	2.03e-37
SynthGas	0.27	-31.04	1.34e-211
Wind	0.04	-12.27	1.29e-34

Table E. 6. Hypothesis test on t-statistics for the output ' VarCFhp'.

Regression input	SE	tStat	p-value
Baseload	0.55	17.40	8.02e-68
DSM	0.46	-4.95	7.42e-07
FossilIndustry	0.01	-38.95	0
Geothermal	0.54	-11.55	7.39e-31
GridStability	0.04	-21.96	6.25e-107
P2H	0.57	171.19	0
Solar	0.05	26.71	3.99e-157
Storage	0.17	-5.56	2.68e-08
SynthGas	0.31	33.18	2.18e-241
Wind_Solar	0.25	10.23	1.39e-24

Table E. 7. Hypothesis test on t-statistics for the output ' VarNatGas'.

Regression input	SE	tStat	p-value
Baseload	0.03	-155.20	0
DSM	0.03	-33.56	3.68e-246
ElecTransport	0.00	-70.21	0
FossilIndustry	0.00	-534.67	0
GridStability	0.00	-335.82	0

Storage	0.01	24.71	1.57e-134
SynthGas	0.02	215.44	0
Wind_Geothermal	0.07	143.74	0
Wind_Solar	0.01	139.17	0

Table E. 8. Hypothesis test on t-statistics for the output 'VarElecDemand’.

Regression input	SE	tStat	p-value
Baseload	0.02	-5.88	4.12e-09
DSM	0.02	897.27	0
FossilIndustry	0.00	660.20	0
P2H	0.02	-7.19	6.72e-13
Solar	0.01	191.02	0
Storage	0.01	-8.52	1.59e-17
SynthGas	0.01	-4.95	7.50e-07
Wind	0.01	187.83	0
Wind_Solar	0.01	-5.18	2.18e-07

APPENDIX F

This appendix shows the slice plots of the outputs analysed. Units: dmnl.

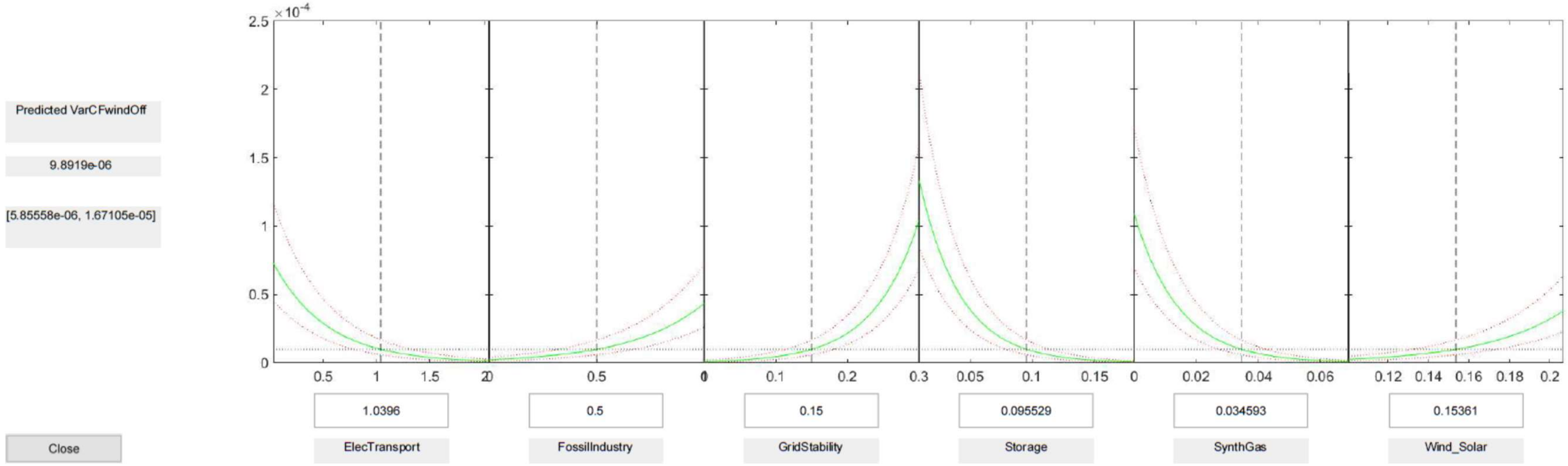

Figure F. 1. Slice plots for "VarCFwindOff"

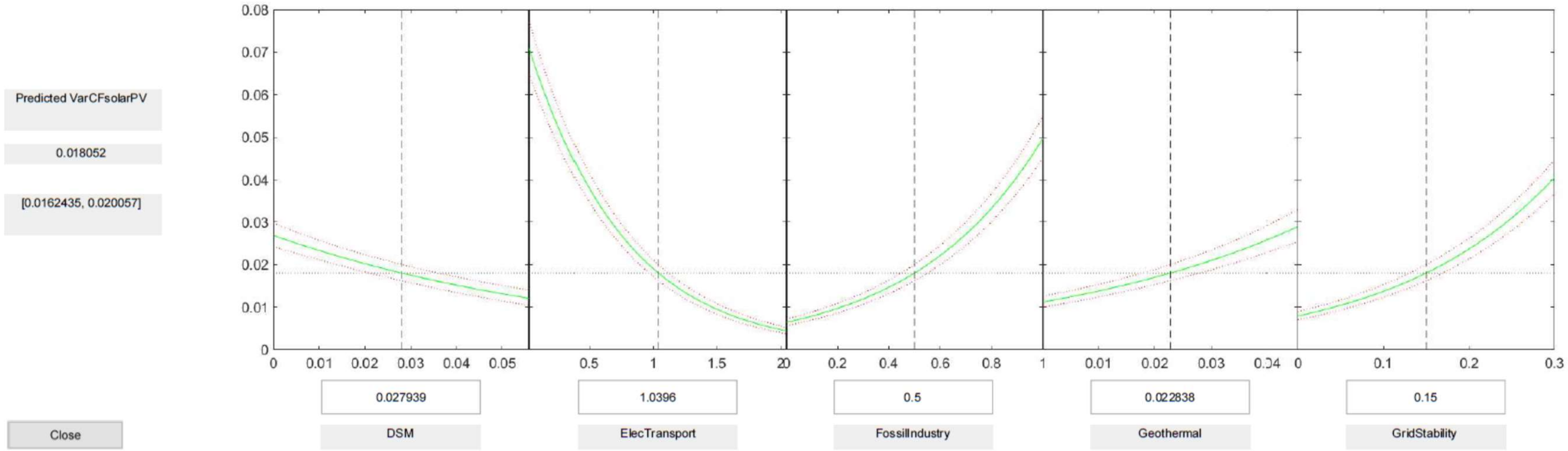

Figure F. 2. Slice plots for "VarCFsolarPV".

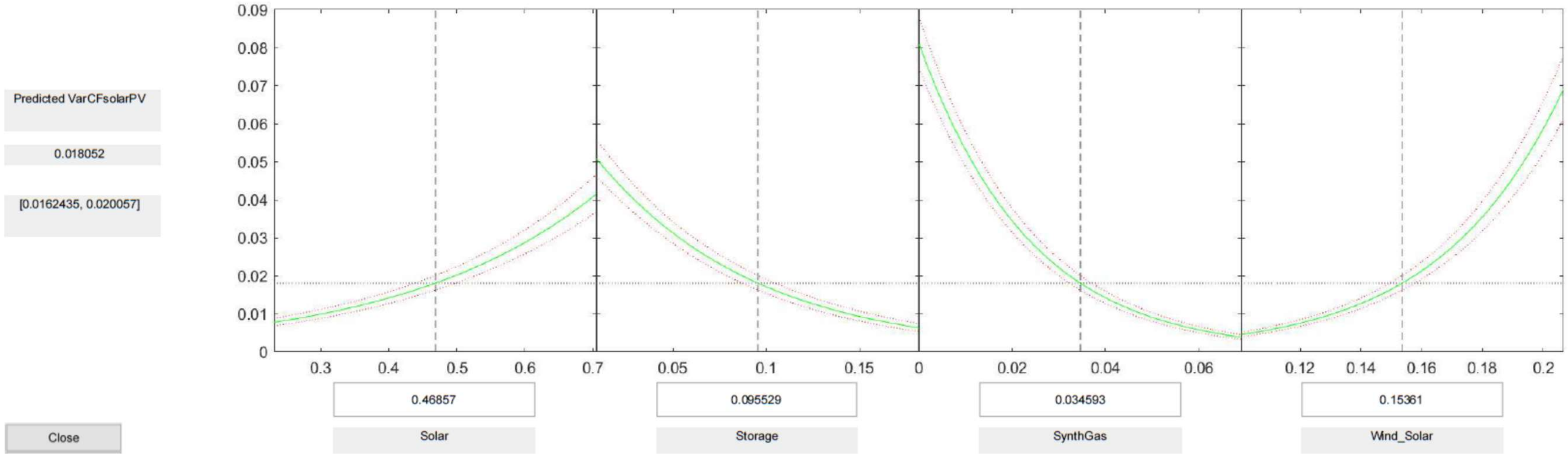

(continued)

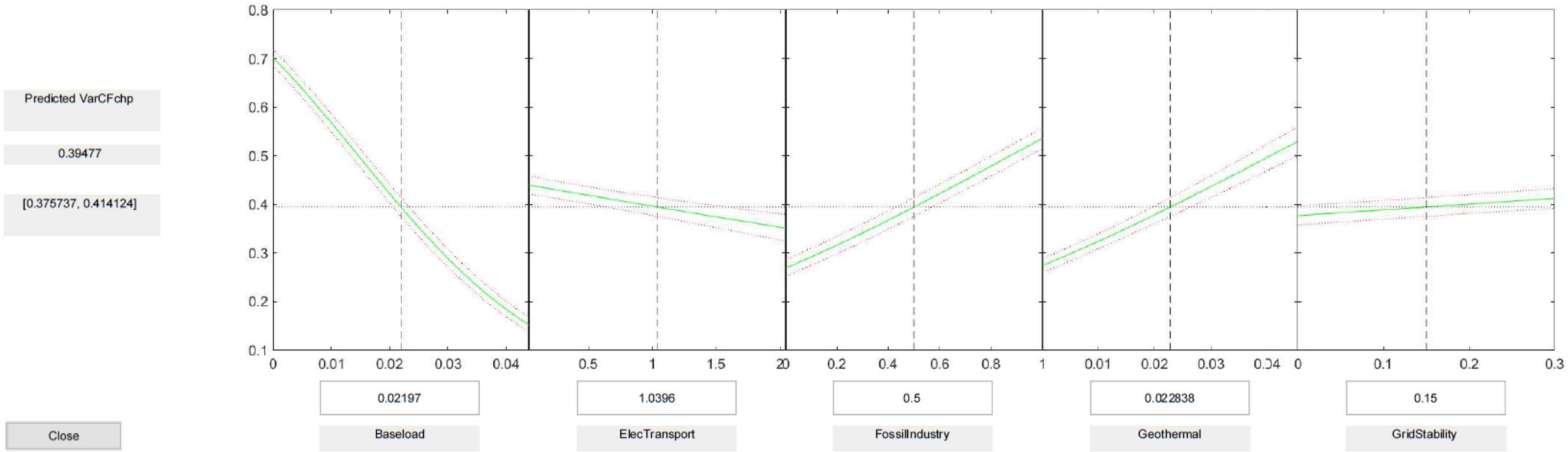

Figure F. 3. Slice plots for "VarCFchp".

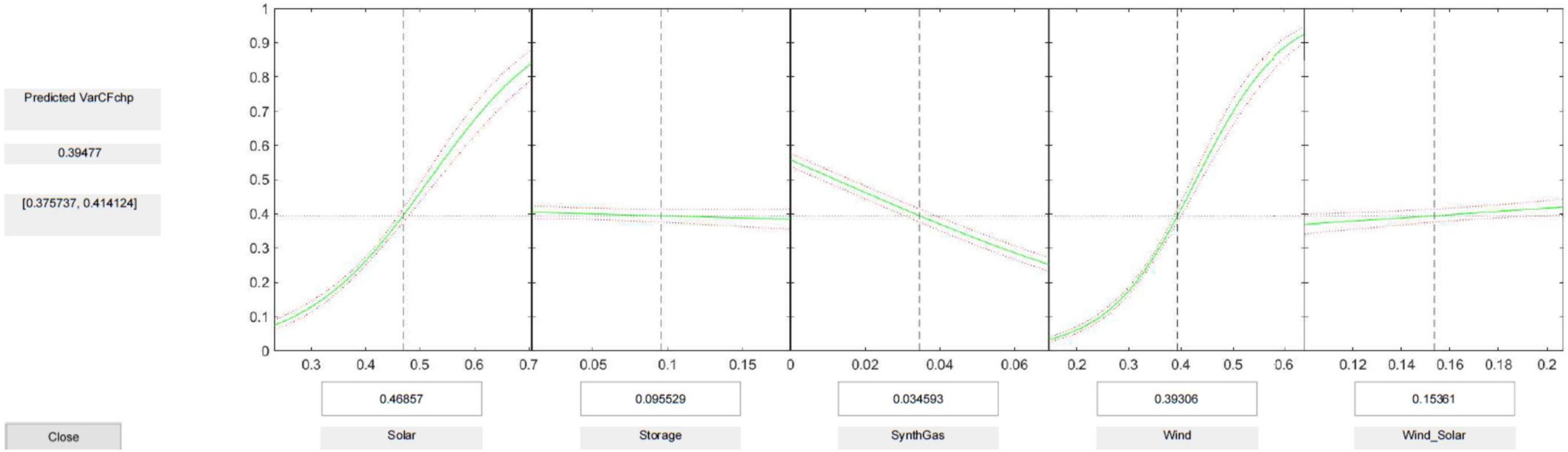

(continued)

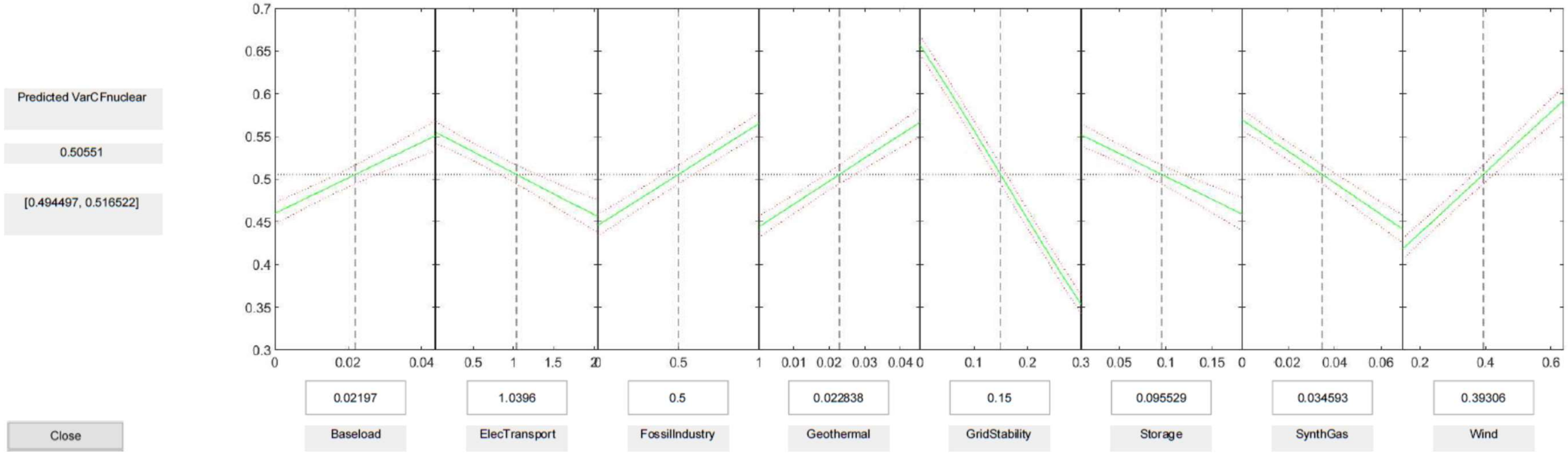

Figure F. 4. Slice plots for "VarCFnuclear".

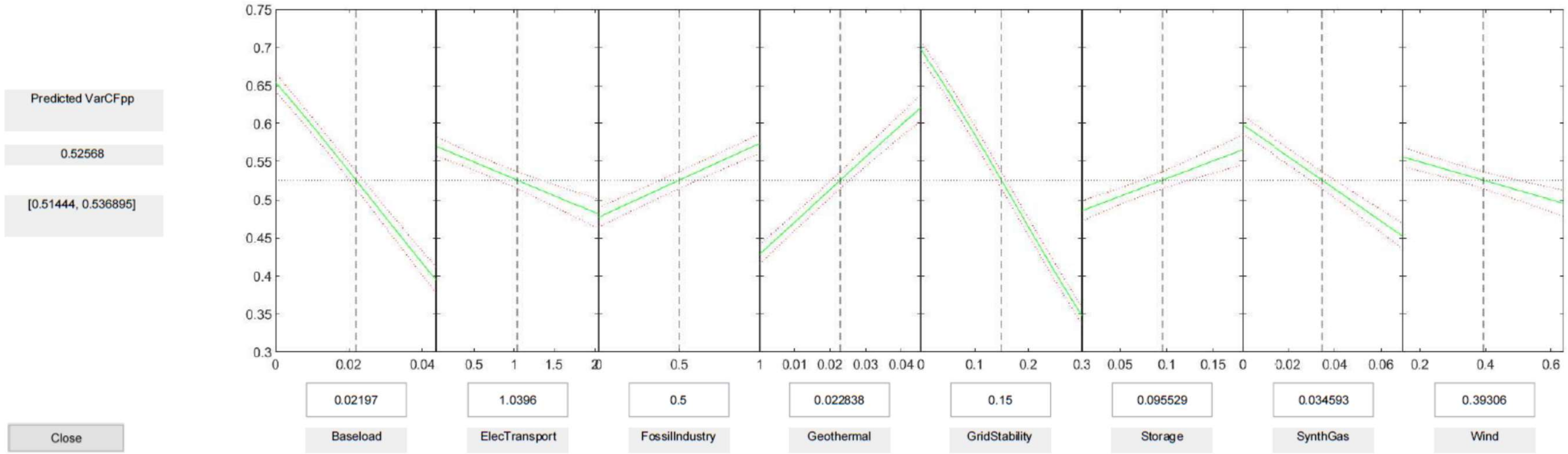

Figure F. 5. Slice plots for "VarCFpp".

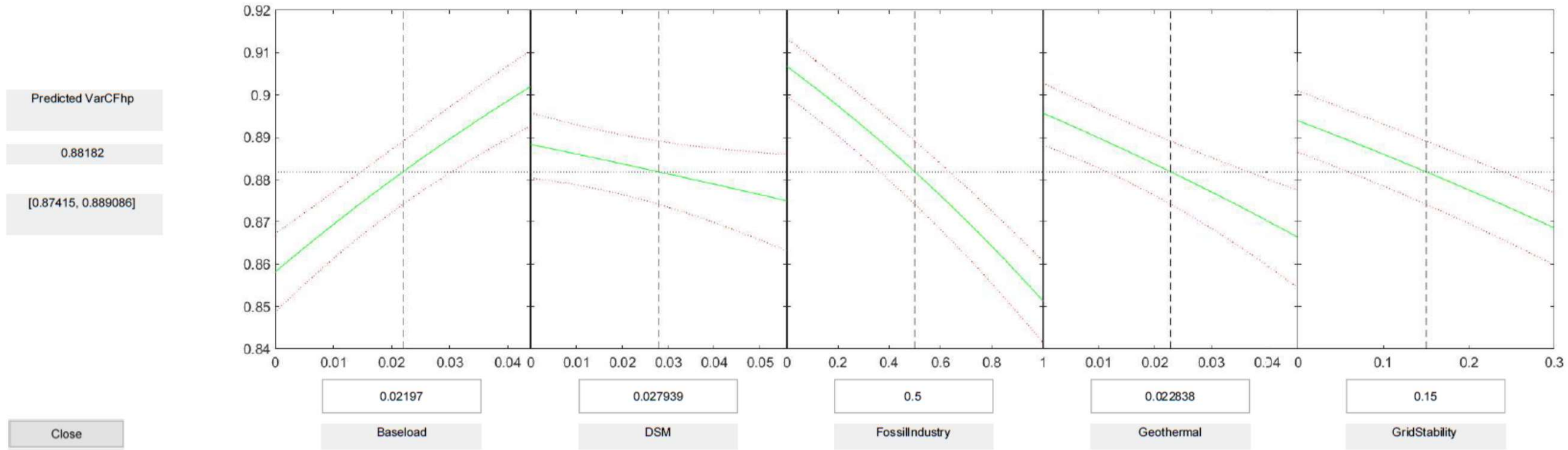

Figure F. 6. Slice plots for "VarCFhp".

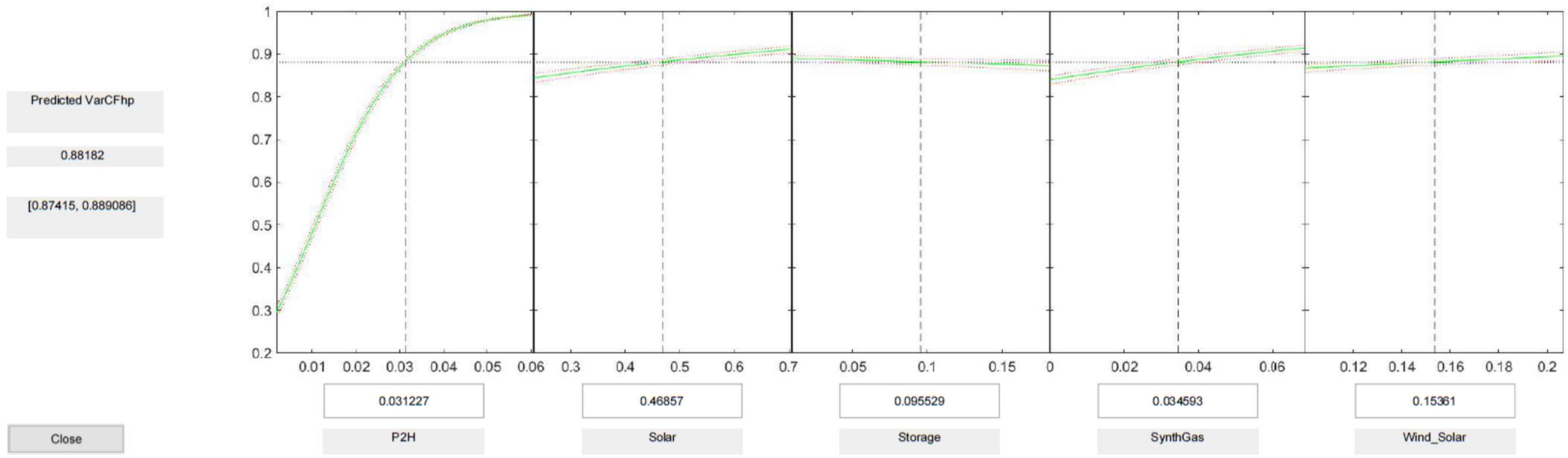

(continued)

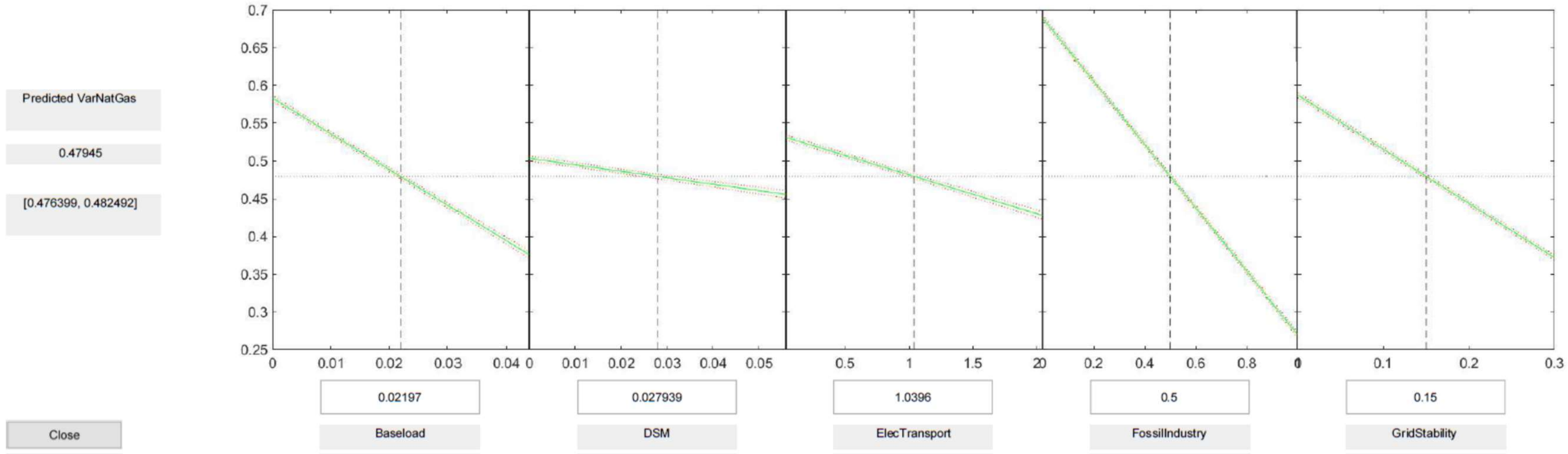

Figure F. 7. Slice plots for "VarNaturalGasDemand".

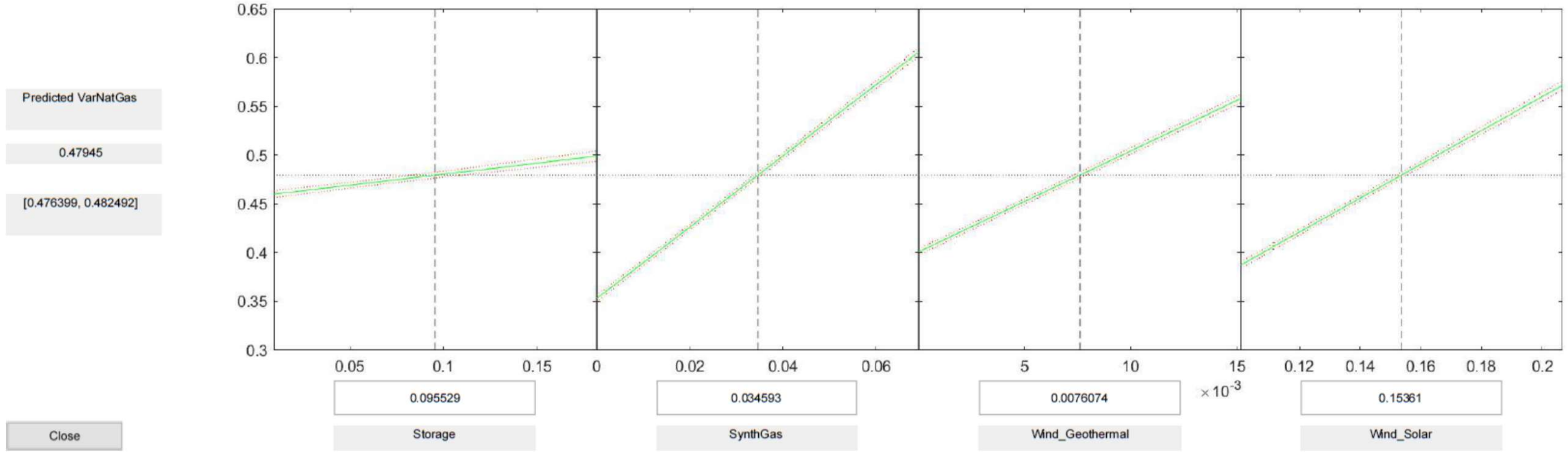

(continued)

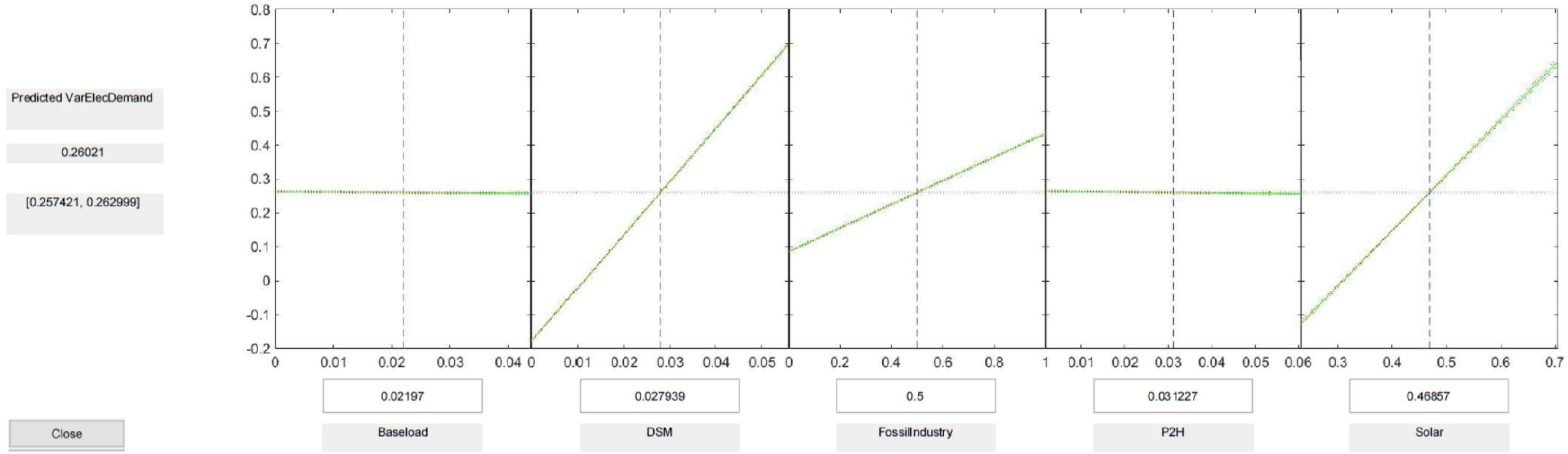

Figure F. 8. Slice plots for "VarNaturalGasDemand".

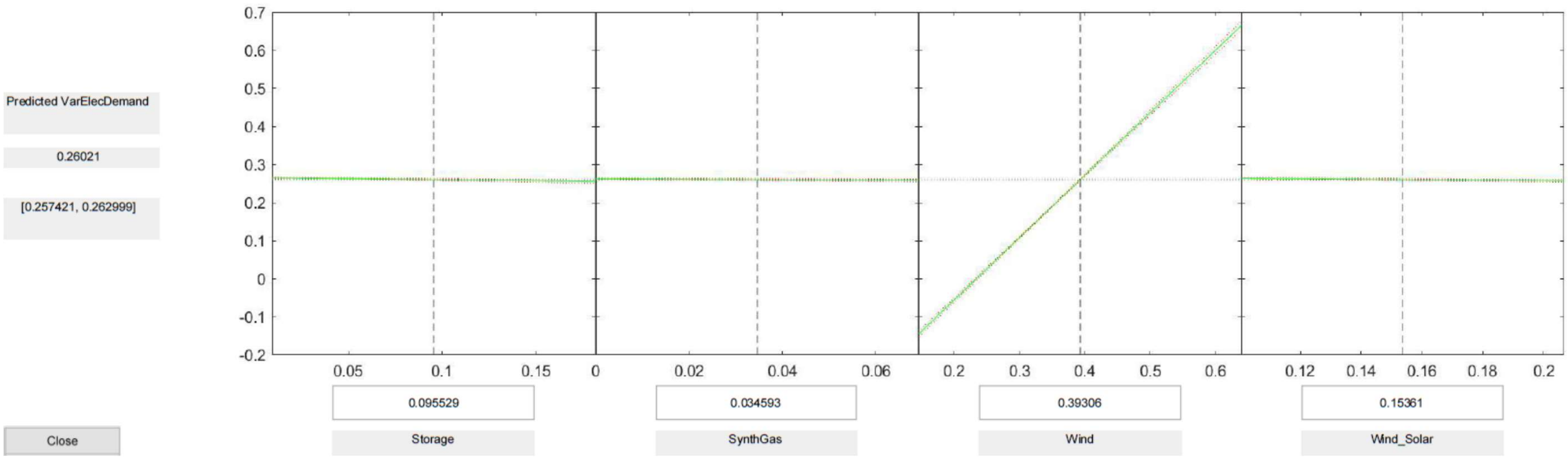
Predicted VarElecDemand
0.26021
[0.257421, 0.262999]
Close
0.095529
Storage
0.034593
SynthGas
0.39306
Wind
0.15361
Wind_Solar

(continued)

APPENDIX G

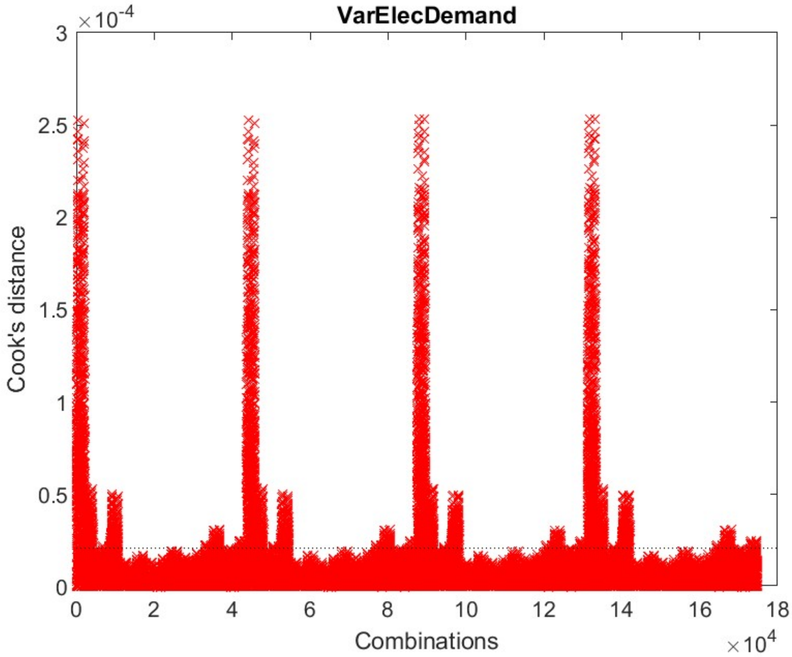

Figure G. 1. Plot observation diagnostics of outliers (Cook’s distance) in MLR model for “VarElecDemand”. The dotted line represents the recommended threshold value of three times the mean.

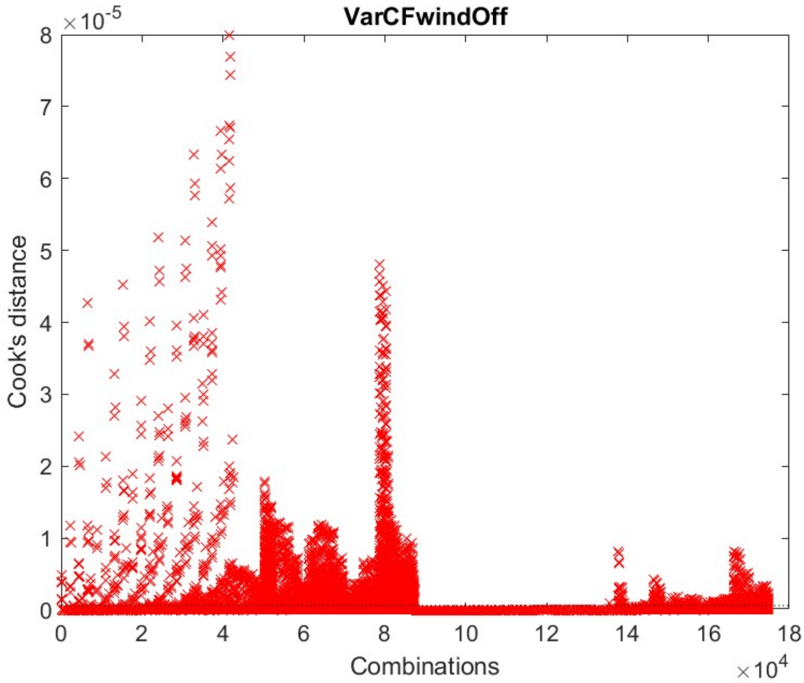

Figure G. 2. Plot observation diagnostics of outliers (Cook’s distance) in MLR model for “VarCFwindOff”. The dotted line represents the recommended threshold value of three times the mean.

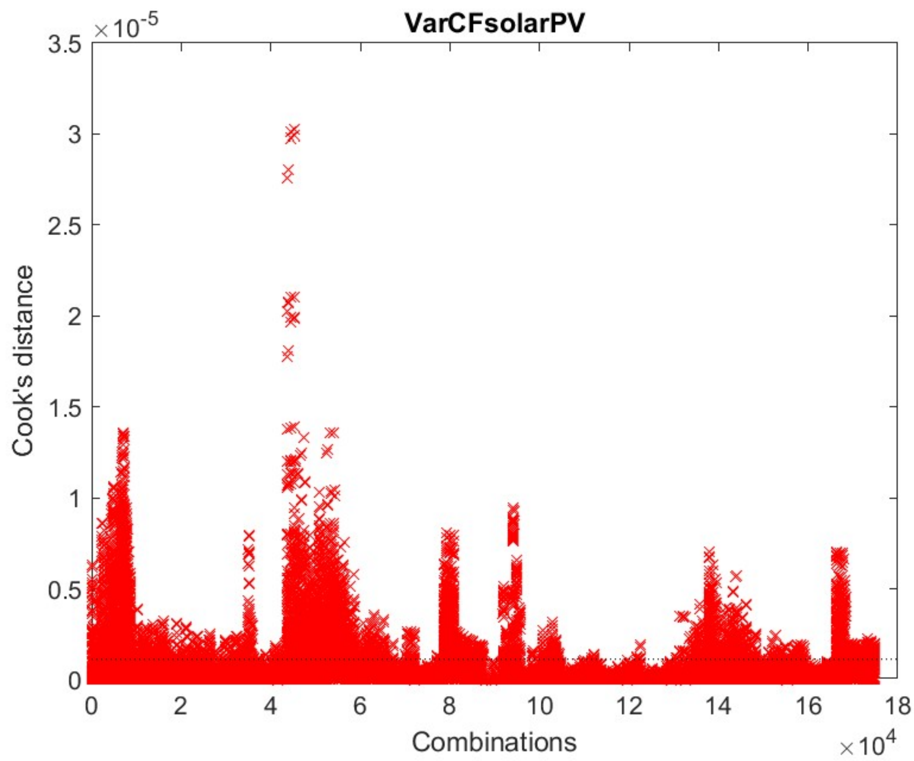

Figure G. 3. Plot observation diagnostics of outliers (Cook's distance) in MLR model for "VarCFsolarPV". The dotted line represents the recommended threshold value of three times the mean.

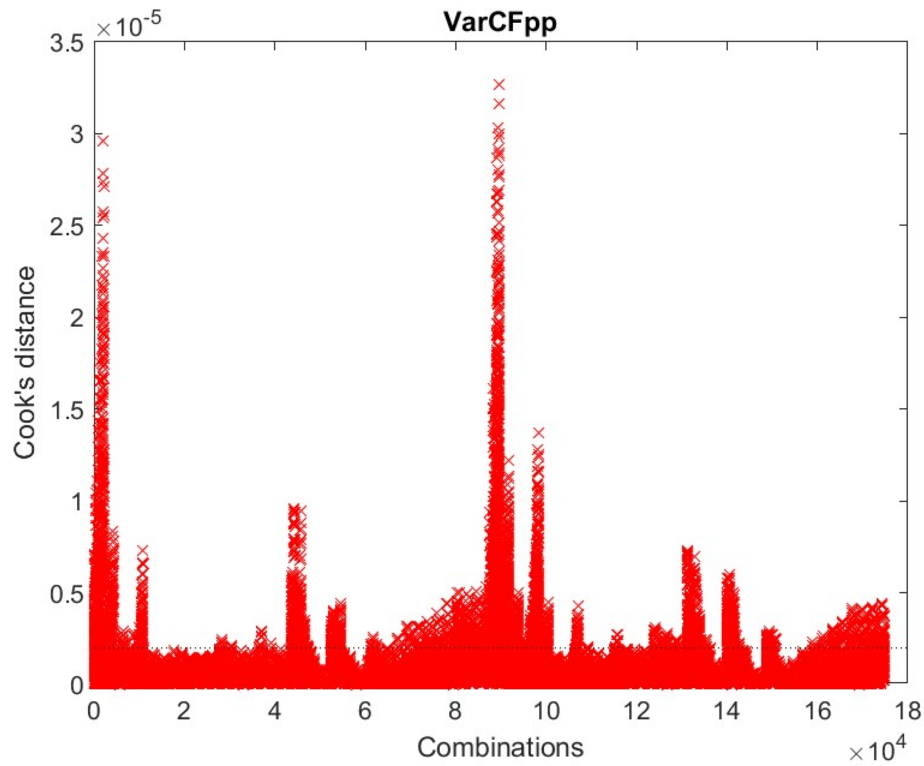

Figure G. 4. Plot observation diagnostics of outliers (Cook's distance) in MLR model for "VarCFpp". The dotted line represents the recommended threshold value of three times the mean.

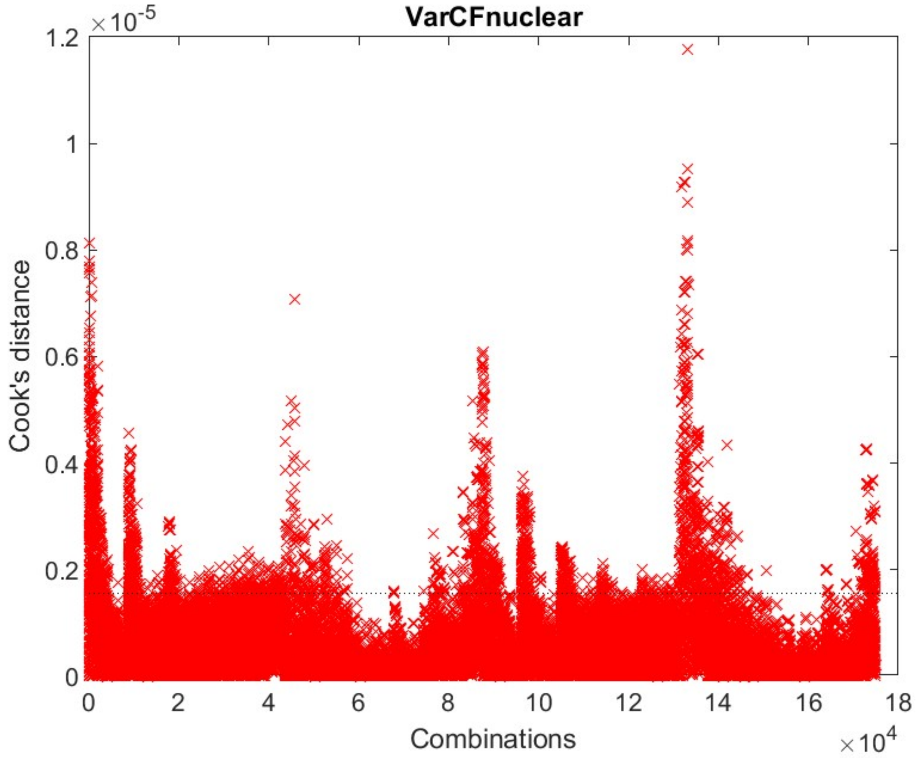

Figure G. 5. Plot observation diagnostics of outliers (Cook's distance) in MLR model for "VarCFnuclear". The dotted line represents the recommended threshold value of three times the mean.

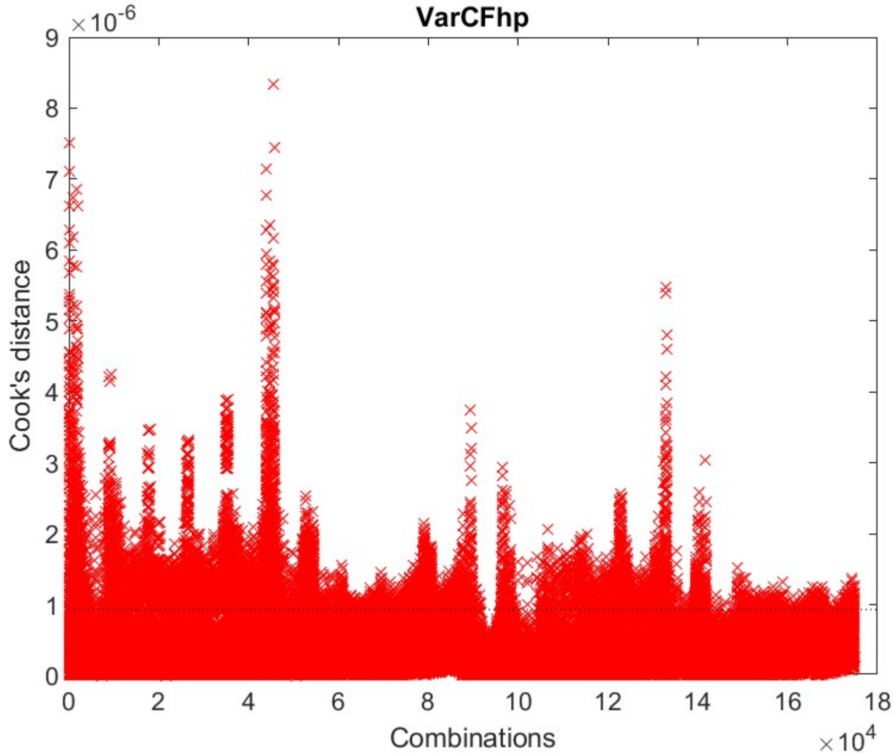

Figure G. 6. Plot observation diagnostics of outliers (Cook's distance) in MLR model for "VarCFhp". The dotted line represents the recommended threshold value of three times the mean.

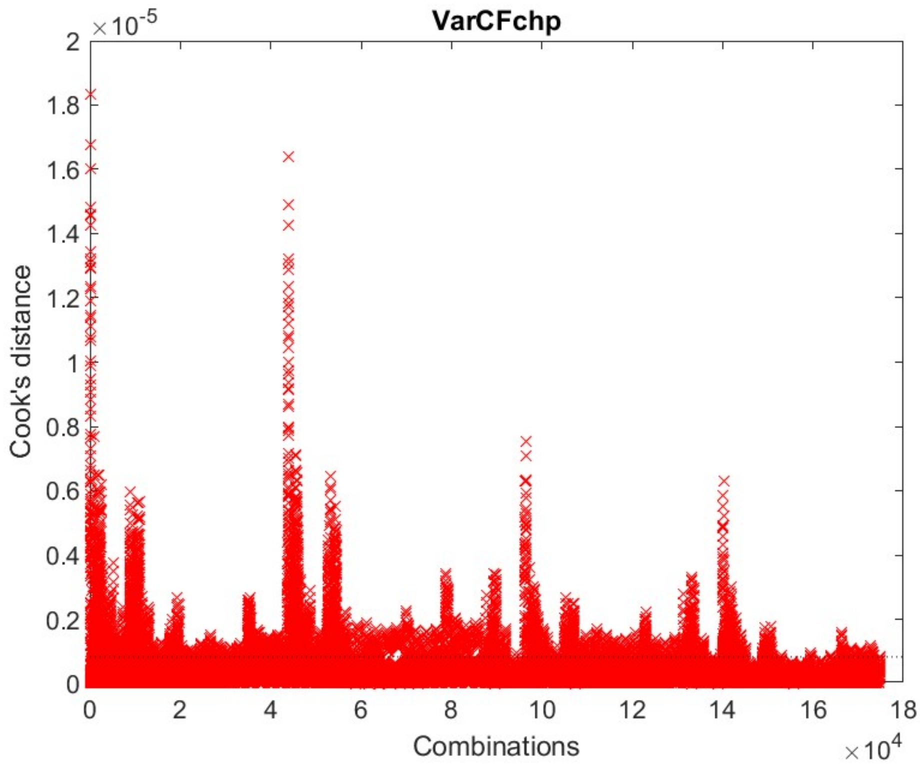

Figure G. 7. Plot observation diagnostics of outliers (Cook's distance) in MLR model for "VarCFchp". The dotted line represents the recommended threshold value of three times the mean.

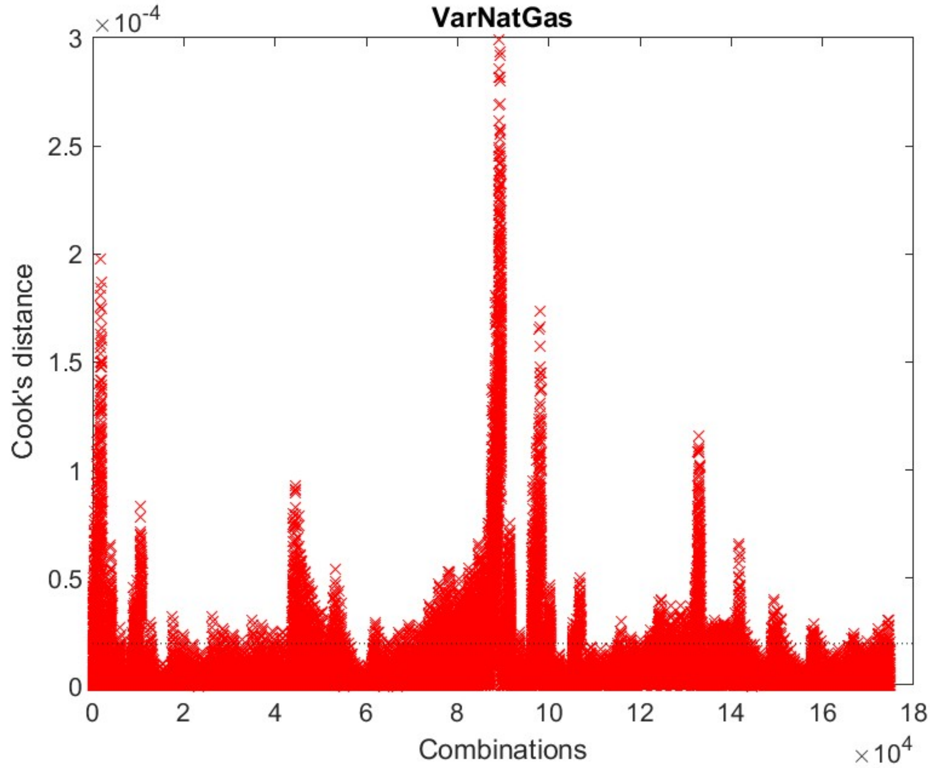

Figure G. 8. Plot observation diagnostics of outliers (Cook's distance) in MLR model for "VarNatGas". The dotted line represents the recommended threshold value of three times the mean.